Spring 2003

A δ18O Calibrated Compartmental Mixing Cell Model of Groundwater Flow in the Roswell Basin, Southeastern New Mexico

Michael M. Gabora

A $\delta^{18}O$ Calibrated Compartmental Mixing Cell Model of Groundwater Flow in the Roswell Basin, southeastern New Mexico

By Michael Gabora

Committee

Dr. Michael E. Campana, Chair
Dr. Zachary Sharp
Dr. Bill M. Fleming

A Professional Project Report Submitted in Partial Fulfillment of the Requirements for the Degree of

Master of Water Resources
Hydroscience Option

Water Resources Program
University of New Mexico
Albuquerque, New Mexico
May 2003

Abstract

For this project fifty-four water samples were collected from sites throughout the Roswell groundwater basin in southeastern New Mexico that were previously sampled by Hoy and Gross in the 1970's. These data sets were used to evaluate the transience of $\delta^{18}O$ values in the basin in hopes of simulating transient conditions with a compartmental mixing cell model. No long-term trend in the data was established. A compartmental mixing cell model was developed and calibrated with the spatial distribution of $\delta^{18}O$. The model was run using the steady-state simulation and produced estimates of groundwater flow paths, volumetric flow rates, recharge rates and residence times. The results estimate the total recharge to the carbonate aquifer as 230,900 afy, slightly lower than previous estimates. Furthermore, the model predicts that 92,400 afy of the recharge to the carbonate aquifer is provided by underflow from deeper units whose source waters originate in the Sacramento Mountains. Mean groundwater ages in the basin ranged from 234 to 924 years and were strongly influenced by the fraction of recharge derived from the underflow component.

Table of Contents

List of Figures

List of Tables

List of Appendices

Acknowledgments

I would like thank my committee for their guidance and support, particularly Dr. Campana who assisted me throughout the project and my graduate education as a whole. I am also very thankful for the assistance of Lin Pan in sorting out some of my modeling kinks. My family has always supported me in my many endeavors including this project and for that am I truly grateful. Lastly, I would like to thank my wife Abby for her constant support, encouragement and companionship. Through temper tantrums at the computer and late nights problem solving at the table she was always there. Without her support the completion of this project would not have been possible. Funding for this project was provided by a University of New Mexico Research Allocations Committee Large Grant, awarded to Dr. Michael E. Campana.

1.0 Introduction

The Roswell Basin underlies approximately 8,000 mi^2 in semi-arid southeastern New Mexico (Figure 1). The groundwater system is comprised of an alluvial aquifer (geographically confined to the Pecos River Valley) underlain by a confined aquifer system whose principal unit is the San Andres Limestone, a karstic limestone deposited during the Permian.

The Roswell Basin is believed to be an ideal location to study the transience of the ratios of deuterium(D)/hydrogen (H) and $^{18}O/^{16}O$ in water molecules and use these data to calibrate a compartmental mixing cell model. Firstly, the basin was the subject of extensive radiogenic and stable isotopic analysis during the 1970's (Hoy and Gross, 1982), which established a sampling network, and a data set with which to compare the newly acquired data. Secondly, the aquifer has been heavily pumped since that time, and one might expect transient isotopic compositions if the groundwater system itself is hydraulically transient. These changes could reflect changes in the source of water being extracted by the pumping well, which in turn may be observable in changes in the isotopic distribution of D/H and $^{18}O/^{16}O$ ratios.

In 1996 Daniel B. Stephens and Associates (DBS&A) completed a groundwater model of the basin using the United States Geological Survey (USGS) finite-difference code MODFLOW (McDonald and Harbaugh, 1988). This model is used by the New Mexico Office of the State Engineer (OSE) to assist in the administration of groundwater rights in the basin. The model (referred to as the OSE model throughout this text) predicts that the bulk of the recharge to the carbonate aquifer is the result of upward leakage from deeper formations, with only minor recharge coming from tributary seepage and diffuse recharge. The

construction and calibration of the compartmental mixing cell model will allow for verification as to whether underflow is the dominant recharge mechanism and provide a validation tool for the OSE model.

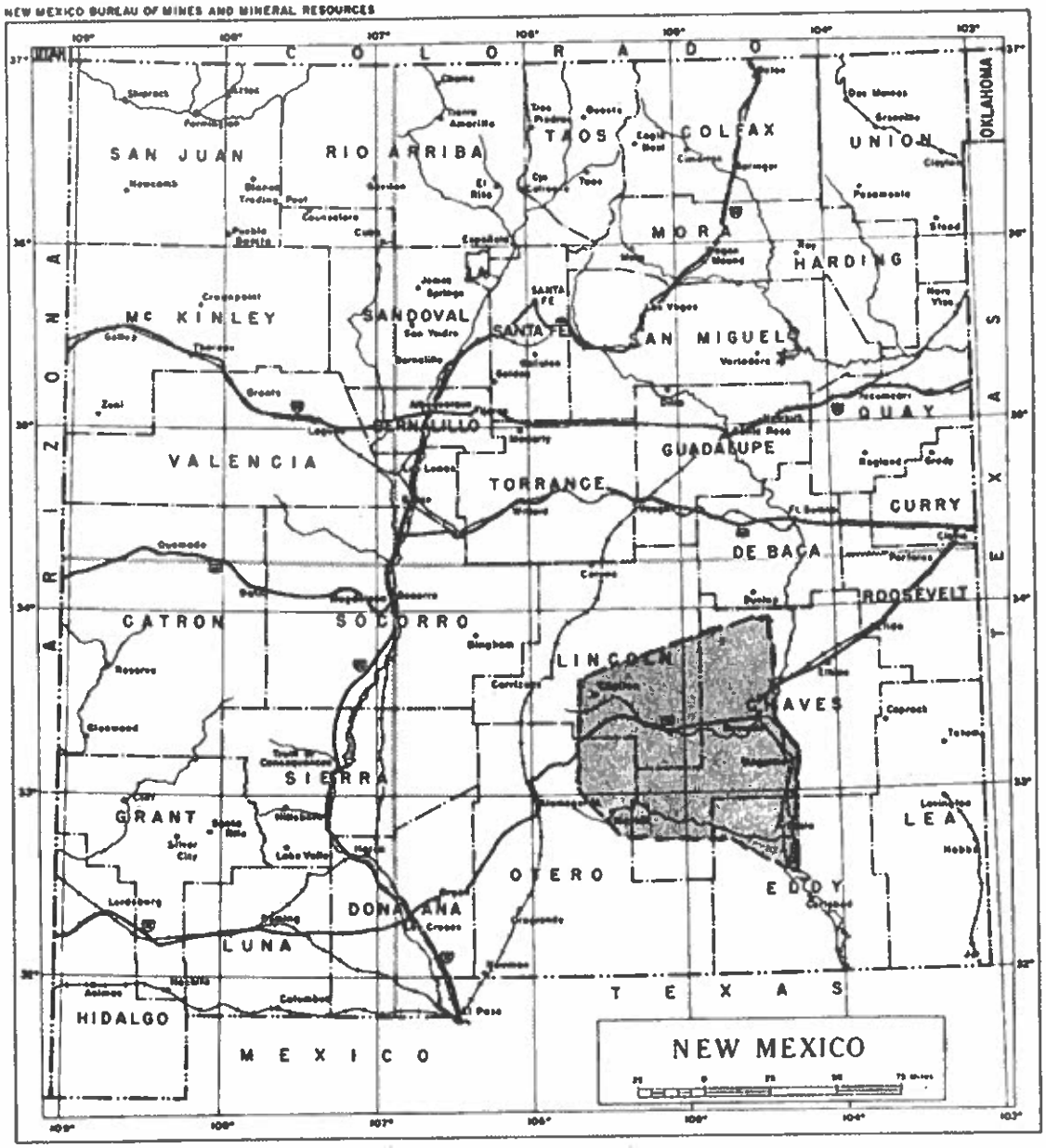

Figure 1. Vicinity map (from Hoy and Gross, 1982)

2.0 Purpose and Scope

The goals of this project were to:

1. Challenge the assumption that subsurface flow systems are steady-state with respect to isotopic composition by resampling some of the locations sampled by Hoy and Gross (1982) and analyzing the water samples for δD and $\delta^{18}O$ values
2. Use the results of the isotopic analyses to calibrate a compartmental mixing cell model to simulate the flow distribution in the Roswell basin
3. Use the raw data and the results of the model to further test the hypothesis that the principal source of recharge to the carbonate aquifer is underflow from the Glorieta Sandstone and Yeso Formations
4. Provide a validation tool for the OSE MODFLOW model

The initial task was to collect fifty-four samples (Figure 2) for isotopic analysis during two field trips, the first in March 2001 and the second in August 2001. Samples were collected from streams, snow pack, and wells completed into the alluvial aquifer, the Glorieta Sandstone and Yeso Formation and from unconfined and confined regions of the carbonate aquifer. These samples were analyzed for δD and $\delta^{18}O$ values in the stable isotope laboratory at the Department of Earth and Planetary Sciences at the University of New Mexico. The data were then compared to previous data in order to assess the degree of transience and then were used to calibrate the compartmental mixing cell model to simulate groundwater flow in the basin.

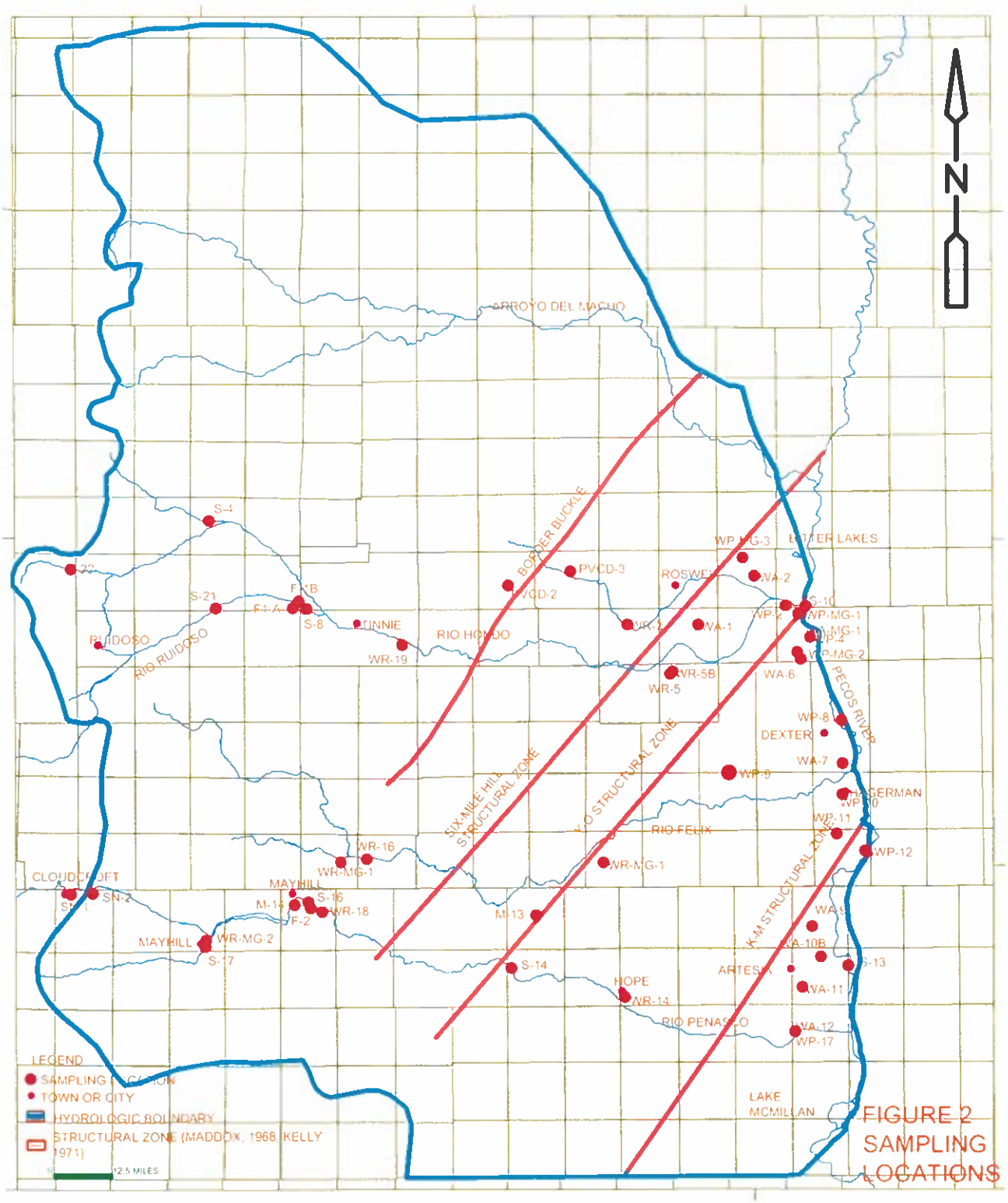

FIGURE 2
SAMPLING LOCATIONS

3.0 Description of Study Area

The Roswell Groundwater Basin is located in southeastern New Mexico and covers an area of approximately 8000 square miles (mi^2). The basin is bounded by the Pecos River Fault to the east, the Sacramento Mountains to the west and by Arroyo del Macho and Seven River Hills to the north and south, respectively. The basin consists of three vastly different physiographic regions (after Gross and Hoy, 1982): the agricultural zone, the principal intake area and the mountain zone (Figure 3).

The agricultural zone includes the 1500 $mile^2$ area along the Pecos River and the City of Roswell. This area has the highest groundwater extraction rates; the majority of the groundwater is used for irrigation. Over 95% of the 360,000 acre-feet/year (afy) of groundwater withdrawals in the basin is used for irrigation (OSE, 1996). The period of irrigation in the area is from April through September; as a result, most groundwater extraction occurs during this period. Wells in this area produce from either the artesian aquifer (carbonate aquifer) or the shallower alluvial aquifer; however, 240,000 afy of the total 360,000 afy are withdrawn from the carbonate aquifer; The average elevation in this area is approximately 3400 feet with a mean annual temperature of 58°F (15°C) and an average annual precipitation of 9.82 inches (DBS&A, 1996).

The principal intake area (Bean, 1949) comprises the 4500 mi^2 area draining the western slope of the mountain zone. The area is principally comprised of sparsely vegetated rangelands with desert flora; however the type of vegetation is controlled principally by elevation and pinion and juniper trees are common at higher elevations. Irrigation is sparse,

FIGURE 3. ROSWELL BASIN LANDSAT

and conducted in areas close to surface water features such as the Rio Felix and the Rio Penasco (Figure 3). Groundwater in this area occurs under unconfined conditions in the San Andres Formation, a limestone characterized by strongly developed solution features. Surface water flows are transmitted rapidly by solution enhanced fractures and is incorporated into the carbonate aquifer directly (Hoy and Gross, 1980). Diffuse recharge in this area also infiltrates and directly recharges the carbonate aquifer. The average precipitation in Hope, NM (Figure 2) is 14.78 inches, which is a good approximation for the zone as a whole.

The mountain zone is comprised of the landmass essentially west of longitude of 105° and is characterized by high desert rangelands and the mountainous areas of the Sacramento Mountains. The mountains serve as the main source of runoff to the tributaries of the Pecos River. The San Andres Formation becomes higher in the stratigraphic sequence (dip east) to the west and the lower members of the formation, the Glorieta Sandstone and the Yeso Formation, become important water producers (Gross et al., 1976). The importance of these units will be discussed in greater detail in section 4.1. Precipitation in this zone varies from 16.4 inches/year in Elk, NM to greater than 20 inches/year in Cloudcroft, NM (Figure 2).

4.0 Hydrogeology

4.1 General hydrogeology

The Roswell groundwater basin has been extensively pumped since the turn of the last century and is currently being mined with respect to groundwater. Based on OSE pumping records the average yearly estimated withdrawals from 1970 to 1983 from the groundwater system were 384,707 afy. The groundwater system is comprised of a shallow unconfined alluvial aquifer in the agricultural zone and a deeper carbonate aquifer that are separated by a thick aquitard as illustrated in Figure 4.

The shallow aquifer is comprised of alluvial fill deposited during the Pliocene, Pleistocene and Holocene on eroded surfaces of east dipping rocks of Permian age (Table 1), such as the Artesia Group (Kelley, 1971). The thickness of the aquifer is varies from 0 at the western margin of the alluvial fill to greater than three hundred feet (Welder, 1983). The hydraulic gradient trends to the east-southeast and is generally steeper in the northern portion of the basin. The alluvial aquifer contributes approximately 18,750 afy to the baseflow of the Pecos River from Acme to Artesia. However, the Pecos River becomes a losing stream from Artesia to Lake McMillian and returns approximately 19,800 afy to the alluvial aquifer (DBS&A, 1996).

The alluvial aquifer is hydraulically connected to the deeper carbonate aquifer through the Artesia Group, a Permian aged aquitard which functions as a semiconfining unit for the carbonate aquifer. The Artesia Group is comprised of five formations: the Tansill Formation, the Yates Formation, the Seven Rivers Formation, the Queen Formation and the basal formation, the Grayburg Formation. The group is comprised of dolomite, sandstone, gypsum,

siltstones and red mudstones (Kelley, 1971). The OSE model (DBS&A, 1996) estimates the overall vertical hydraulic conductivity of the Artesia Group to be $3*10^{-4}$ to $5*10^{-7}$ ft/d.

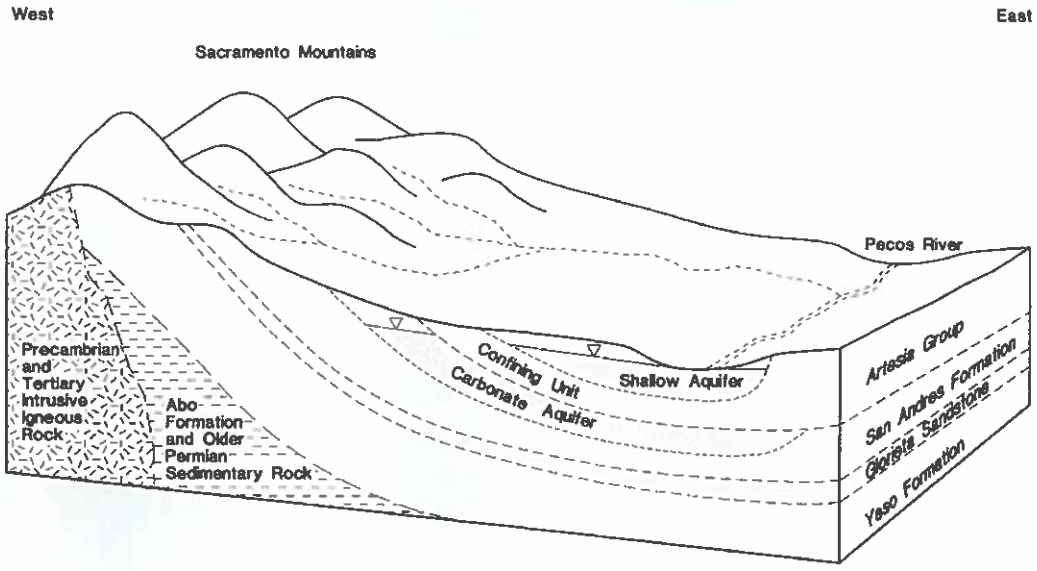

Figure 4. Schematic cross-section of the Roswell Basin, New Mexico (modified from DBS&A, 1996)

Age		Formations & Members		Thickness (ft)	Description
Holocene and Pleistocene			Assorted surficial deposits	0-300	Valley alluvium, terrace and pediment gravel, caliche soils, aeolian sand, travertine
Pleistocene-Pliocene			Gatuna Formation	0-200	Sandstone, sand gravel, siltstone, limestone, red, brown, tan, gray, yellowish
Permian	Guadalupian Series	Artesia Group	Tansill Formation	200-300	Dolomite and siltstone (south); dolomite, gypsum, and anhydrite (north)
			Yates Formation	250-350	Siltstone, sandstone, dolomite, limestone, and gypsum (south); gypsum, siltstone, and thin dolomite (north)
			Seven Rivers Formation	450-600	Dolomite, siltstone (south); gypsum and siltstone (north)
			Queen Formation	200-400	Dolomite and sandstone (south); gypsum, red mudstone, dolomite (north)
			Grayburg Formation	250-450	Dolomite and sandstone (south); gypsum, mudstone, dolomite (north
	Leonardian Series		San Andres Formation:		
			Fourmile Draw Member	0-700	Dolomite, gypsum, reddish mudstone; sandstone locally at top; thin-bedded
			Bonney Canyon Member	0-300	Dolomite, local limestone; gray, light-gray, local black; thin-bedded
			Rio Bonito Member	250-350	Dolomite, limestone; gray, brownish gray; thick-bedded
			Glorieta Member	125-150	White to yellowish, fine-grained, subangular to subrounded, well sorted, friable sand
			Yeso Formation	0-2,400	Sandstone, siltstone, dolomite, gypsum; tan, red-yellow, gray, white

Modified from Kelley, 1971.

Table 1. Stratigraphy of the Roswell Basin (from DBS&A, 1996)

The higher reported values are associated with structural features such as the K-M structural zone.

The San Andres Formation is an east-dipping Permian aged karstic limestone interbedded with dolomite, gypsum and some mudstones. It serves as the principal aquifer for the basin and will for the remainder of this paper be termed the carbonate aquifer. The basal member of the Formation, the Glorieta Member, is a yellowish, fine-grained, well-sorted sand.

The majority of water flow in the San Andres occurs in the upper 50-75 feet of the formation (Welder, 1983), where extensive dissolution of evaporite, and carbonate interbeds, along fractures and bedding planes has greatly enhanced the ability of the formation to store and transmit water. The carbonate aquifer is unconfined to the west of 105°30' (approximately) and confined east of 105°30'. The significant confining pressures east of 105°30', result in upwards leakage of groundwater through the Artesia Group to the alluvial aquifer. However, as a result of extensive pumping of the aquifer during the irrigation season, a reversal in the vertical gradient can allow for ground water from the alluvial aquifer to leak into the carbonate aquifer (Hoy and Gross, 1982, DBS&A, 1996).

Previous investigators have attempted to quantify the transmissivity of the carbonate aquifer. Rehfeldt and Gross (1982) estimated the transmissivity in the north central portion of the basin to be 250,000 ft^2/d. DBS&A (1996) calculated a range of values for the basin from 1,000 ft^2/d to 300,000 ft^2/d, with the highest values also occurring in the north central portion of the basin, likely the result of structural features, which substantially increase the secondary permeability. Generally, the transmissivity is lower to the southeast, particularly southeast of

the Y-O structural zone. The storage coefficient of the aquifer is estimated to be 0.05 in the unconfined portion and 0.0005 in the confined portion of the formation (DBS&A, 1996).

The San Andres Formation is underlain by the Yeso Formation, a thick sequence (0-2,400 ft) of sandstone, siltstone, dolomite and gypsum (Kelley, 1971). While the formation was initially thought to be a poor aquifer (Mourant, 1963), however, more recent work suggests that the transmissivity of the formation is substantial (Wasiolek, 1991, DBS&A, 1996). Bean (1949) suggests that the permeability of the Yeso Formation is likely greatest in the northern portion of the basin as a result of the evaporite sequences within the Yeso Formation in this area. The lateral inflow from the Glorieta Member and Yeso Formation to the carbonate aquifer is estimated to be 54,000 afy (DBS&A, 1996). This estimate is based on the length of the contact, the estimated transmissivity of the formation and the observed hydraulic gradient. These formations are believed to also contribute significant recharge to the carbonate aquifer by a deeper, upward-leakage mechanism that will be discussed in detail in section 4.2.

4.2 Recharge mechanisms

Previous investigators (Gross and Hoy 1980, Gross, 1982) have suggested that the carbonate aquifer has three natural recharge mechanisms: a slow component comprised of upward leakage from the Glorieta Member and Yeso Formation, a fast recharge component from stream channels and arroyos, and a minor component comprised of diffuse recharge from precipitation. These mechanisms are illustrated by Figure 5.

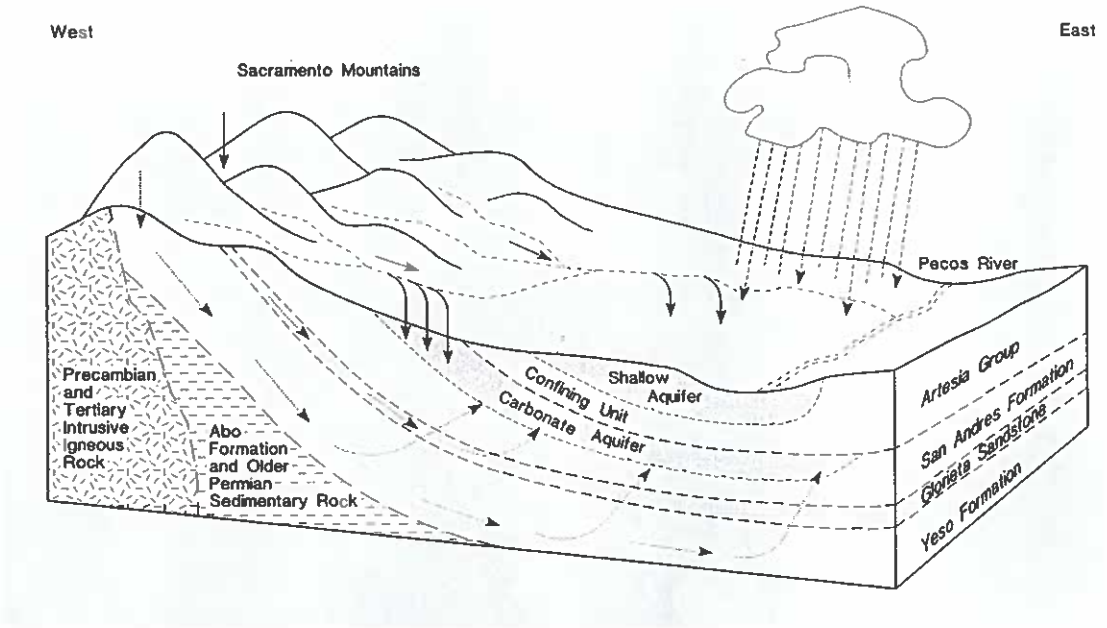

Figure 5. Illustration of recharge mechanisms proposed by Hoy and Gross (1980)(modified from DBS&A, 1996)

Tritium analyses performed by Gross (1980) at numerous sampling points in the Roswell Basin (including many of the locations used in this study) have played a major role in deciphering the recharge components of the basin. The samples collected from wells located near streams, particularly the Rio Hondo, suggest that local recharge is occurring rapidly, as evidenced by high tritium activities near the stream. In contrast, samples collected farther from the stream had very low tritium activities. This suggests that local recharge is occurring near the streams in the recharge area and that some other method of recharge (which proceeds at slower rates) is occurring in other portions of the aquifer.

The majority of the recharge from streams in the basin occurs from the Rio Hondo, Rio Penasco, and Rio Felix; however, large precipitation events likely result in recharge from ephemeral tributaries of the Pecos River. This is further supported by the experiments performed by Fielder and Nye (1933) along the Rio Hondo and the Rio Penasco, which suggest that both streams lose significant amounts of water through the principal intake area.

It also seems likely that the secondary permeability created by the Six-Mile Hill and Y-O structural zones may act as a conduit for increased channel loss resulting in enhanced recharge through these reaches (Bean, 1949).

While Fielder and Nye (1933) acknowledged that the confining pressures in the Yeso were great enough to produce upward leakage into the San Andres Formation, they did not believe that sufficient water was present in the Yeso to provide a significant quantity of recharge. However, as discussed previously, more recent work (Rehfeldt and Gross, 1982, DBS&A, 1996) suggests that the Yeso has significant permeability in portions of the formation and carries enough water to be a significant recharge component to the San Andres Formation. Wasiolek (1981) suggests that the Yeso Formation transmits water through a series of highly permeable layers separated by low permeability layers. These high permeability layers appear to be laterally extensive and the water being transmitted in these confined layers is under considerable pressure. The results of pumping tests on the Mescalero Reservation produced transmissivities ranging from 18 to 5,900 ft^2/d and hydraulic conductivities ranging from 0.1 to 92 ft/d (Wasiolek, 1991). Wasiolek (1981) also suggests that the Six Mile Hill and Y-O structural zones could provide the necessary pathway for water to leak upward from the Yeso Formation and Glorieta Member to the San Andres Formation. Childers and Gross (1985) suggested that the porosity of the Yeso Formation decreases substantially east of the Y-O structural zone (where the aquifer becomes confined, see Figure 2), suggesting that water flowing from west to east encounters progressively less permeable material (thereby increasing the gradient in the vertical dimension).

Based on a water balance for the basin Rehfeldt and Gross (1982) suggested that due to the small volume of recharge originating as diffuse recharge from precipitation (16% to

20%) and the volume of recharge needed to reproduce the observed pressure heads in the San Andres Formation that upward leakage from the Yeso Formation and Glorieta Member must be contributing more than 50% of the total recharge. This hypothesis was supported by results of the Rehfeldt and Gross numerical mixing cell model (modeling only a small area in the north central portion of the basin) using tritium activities.

The hypothesis is further supported by the most recent work in the basin, the OSE model, that predicts that over 50% of the recharge to the groundwater system is a result of upward leakage from the Glorieta Member, the basal member of the San Andres Formation, and the Yeso Formation. Allowing for a substantial amount of flow to recharge the carbonate aquifer through upward leakage from the Yeso Formation was essential in order to achieve calibration of the model.

The conceptual model (as illustrated in Figure 5) initially suggested by Gross (1982) and supported by more recent work is that precipitation originates on the western slope of the Sacramento Mountains and is transmitted through the Yeso Formation and Glorieta Member. A small portion is laterally transmitted to the carbonate aquifer, and a greater portion flows down dip and subsequently leaks upward through faults or primary permeability from the Yeso Formation to the San Andres Formation as a result of the high confining pressures. However, other processes are believed to be components of the slow recharge component. These processes included spring discharge that feed principally from the Yeso Formation (older water), and subsequently discharge into channels, after which water is recharged through the losing reaches of the channel (Gross and Rehfeldt, 1979).

Two additional recharge mechanisms are the result of decreasing heads in the carbonate aquifer during the pumping season. The decrease may result in a gradient reversal

from upward leaking to downward leaking from the alluvial to the carbonate aquifer. This causes water in the shallow aquifer derived from Pecos River water and irrigation returns to leak into the carbonate aquifer. Additionally, the decrease in the potentiometric surface is likely responsible for the saltwater intrusion northeast of Roswell that is associated with evaporite sequences in the San Andres Formation (Gross and Hoy, 1980).

4.3 Quantification of recharge

Previous investigators have attempted to quantify recharge to the Roswell Basin with a variety of methods. Fielder and Nye (1933) estimated groundwater discharge to the Pecos River from all known sources prior to development as 235,200 afy. Hantush (1957) plotted the discharge for the basin (pumping rates, spring flow and baseflow) against the three-year average rainfall for three years in which he considered the system to be in a dynamic equilibrium. It was his conclusion that the recharge for 1941 through 1953 averaged 257,000 afy in the carbonate aquifer, and 30,000 afy in the alluvial aquifer, for a total of 287,000 afy.

Additional estimates are provided by Saleem and Jacob (1971) who estimated recharge in the carbonate aquifer to be 240,000 afy from 1903 to 1968. Summers (1972) provides estimates based on stream gauge data on the Pecos River. By using a water balance approach Summers estimated that the natural recharge to the alluvial aquifer to be 42,200 afy and 231,900 afy for the carbonate aquifer, for a total of 274,100 afy. These estimates are relatively consistent with the OSE model that predicts a total natural recharge of 298,934 afy, of which approximately 245,000 afy recharges the carbonate aquifer. Of the roughly 245,000 afy of recharge to the carbonate aquifer, 74% is believed to be derived from Yeso Formation leakage, 16% from precipitation and 10% from tributary seepage.

5.0 Isotope hydrology

5.1 Introduction

Hydrologists have been using the stable isotopes of hydrogen and oxygen for some time as a means of determining characteristics of hydrologic systems such as sources of recharge, degree of mixing, etc. (Campana, 1975; Kirk and Campana, 1990). This is possible because the isotopic composition of water varies with differing physical conditions; for example, during condensation the isotopic composition is determined by temperature and source. Therefore, it is possible to delineate water formed at a warmer temperature from water formed at a colder temperature as a result of this fractionation.

Fractionation results from a preference of one isotope over another isotope of a particular element, resulting from mass differences. These mass differences are a result of the presence or absence of extra neutrons in the nuclei of the isotope (Figure 6).

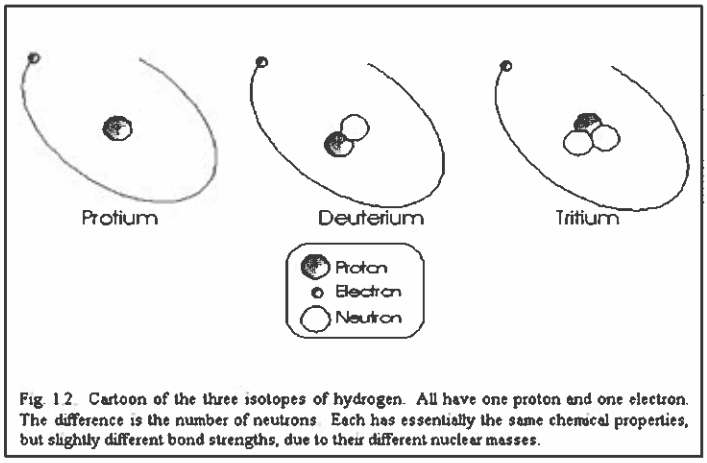

Fig. 1.2. Cartoon of the three isotopes of hydrogen. All have one proton and one electron. The difference is the number of neutrons. Each has essentially the same chemical properties, but slightly different bond strengths, due to their different nuclear masses.

Figure 6. Illustration of the three isotopes of hydrogen (from http://syllabus.syr.edu/GOL/disiegel/Gol400_600/isotopes.ppt)

Two elements have been considered in this study, hydrogen and oxygen, each of which has three isotopes. For hydrogen these are ^{1}H, ^{2}H, ^{3}H (Tritium or T) and for oxygen these are ^{16}O, ^{17}O, and ^{18}O. Because of the small concentration of water molecules containing ^{17}O, due to the small natural abundance of ^{17}O, these molecules are not considered as part of

this study. Tritium is a radioactive isotope of hydrogen and was not used in this study. Therefore, four isotopomers were considered. The four isotopomers and their average natural abundance are summarized in Table 1.

Table 2. Natural abundance of isotopomers

Isotopomer	Average Abundance, %
$H_2{}^{16}O$	99.615
$H_2{}^{18}O$	0.2036
$HD^{16}O$	0.03108
$HD^{18}O$	0.0000006

The isotopic composition of water is expressed in comparison to the isotopic composition of Standard Mean Ocean Water (SMOW) (Craig, 1961). The isotopic composition of water is determined by mass spectrometry and expressed in per mil (‰) deviations from the SMOW standard. These deviations are expressed as δD and $\delta^{18}O$ and are calculated in the following manner (example for $\delta^{18}O$):

$$\delta^{18}O = \left[\frac{\left({}^{18}O/{}^{16}O\right)_{sample} - \left({}^{18}O/{}^{16}O\right)_{SMOW}}{\left({}^{18}O/{}^{16}O\right)_{SMOW}}\right] \times 10^{3}$$

Therefore a sample that has a lower $^{18}O/^{16}O$ than SMOW has a negative $\delta^{18}O$ and a sample with a $^{18}O/^{16}O$ greater than SMOW has a positive $\delta^{18}O$.

5.2 The meteoric water line

In 1961 Harmon Craig published a diagram on which the isotopic analyses of approximately 400 water samples from rivers, lakes and precipitation from various countries were plotted. The diagram illustrated a remarkably linear correlation between the δD‰ and $\delta^{18}O$‰ values along a best-fit line of $\delta D = 8\delta^{18}O+10$ (Figure 7). This line came to be known as the global meteoric water line (GMWL). The line represents a weighted average of local meteoric water lines (LMWL) having slopes less than 8 and whose intercepts vary widely from –2 to +15.

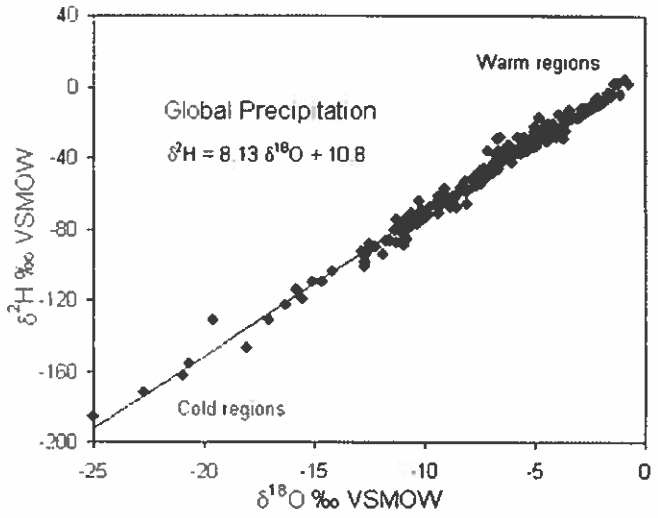

Figure 7. Meteoric water line (as modified by Rozanski et al., 1992, from http://syllabus.syr.edu/GOL/disiegel/Gol400_600/isotopes.ppt)

Generally, analyses of meteoric waters from closed basins or very dry areas lie to the right of the GMWL as a result of kinetic isotope effects or moisture deficits during condensation (discussed in section 5.4). The area to the left of the GMWL is known as the "forbidden zone" because no meteoric water samples plot in this area. While there are a few exceptions to this rule, these samples are very unique and are generally associated with basal brines.

5.3 Deuterium excess parameter

While using an intercept of 10 for the GMWL results in a good correlation for modern worldwide samples, some variation in this value does occur. This results from the fact that the kinetic effects associated with evaporation are a function of the relative humidity near the evaporative surface. The value of 10 ‰ used in the GMWL correlates to the mean relative humidity over the oceans of 82%. Therefore, variations in the deuterium excess parameter arise from variation in the moisture deficit (1-humidity, where humidity is expressed as a decimal). For example, samples from the eastern part of the Roswell Basin, where very arid conditions persist, will have a larger deuterium excess parameter than in the western mountains, as a result of the larger moisture deficit created by the low relative humidity. However, a similar shift in the deuterium excess factor could result from a secondary fractionation such as water that been evaporated during ponding or infiltration.

5.4 Condensation and evaporation

An understanding of the effects of condensation and evaporation on the isotopic composition of water molecules is critical to evaluating variations in the isotopic composition of water in the basin. The process of evaporation is a kinetic process and the factors governing the fractionations associated with this process are quite complex. Alternatively, condensation is an equilibrium process and the fractionations associated with this process are based solely on temperature.

The process of evaporation is especially important in depletion of the light isotopes in surface waters, irrigation return flows and diffuse recharge components of the hydrologic system. Because the vapor pressures of the different isotopomers decrease with increasing molecular weight, lighter isotopomers are more likely to preferentially escape a water body

and enter the vapor phase. Because evaporation is a unidirectional process at low vapor pressures, very little exchange occurs back from the departing vapor to the remaining liquid. Air flow typically moves the vapor before a dynamic equilibrium of exchange between the vapor phase and the liquid phase can occur.

It is this failure to achieve complete isotopic exchange between the liquid and the vapor phases that results in the water vapors above the ocean having lighter $\delta^{18}O$ values than would be expected based on the equilibrium fractionation factor at the temperature of the ocean. Therefore, the average vapor over the oceans is approximately –13 ‰, rather than -9‰ (as predicted by known equilibrium isotopic fractionation).

This disequilibrium effect is less pronounced for hydrogen because the mass difference between the two isotopomers $HD^{16}O/H_2{}^{16}O$ is significantly less than the mass difference between $H_2{}^{18}O/H_2{}^{16}O$. Therefore, residual water that has been exposed to evaporative processes will become more enriched in ^{18}O than ^{2}H. This difference in the slope of the δD versus $\delta^{18}O$ as compared to a LMWL can be used to identify the waters that have been exposed to evaporative processes.

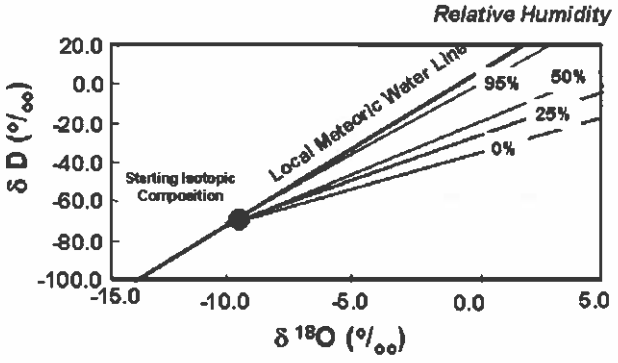

Figure 8. Evaporative enrichment in δD (from http://sylabus.syr.edu/GOL/disiegel/Gol400_600/isotopes.ppt)

When an air mass becomes saturated with water vapor, condensation will occur. In contrast to evaporation, during condensation the heavier isotope is preferentially removed, resulting in the parent vapor becoming isotopically lighter. Condensation is best represented by a Rayleigh type isotopic fractionation, whereby the liquid condensate is in isotopic equilibrium with the water vapor. While Rayleigh conditions rarely occur in nature (due to exchange between water vapor and condensate in clouds), it is the best conceptual model of condensation. Essentially, in this model condensate is continually removed from an air mass, resulting in the remaining water vapor in the air mass becoming more depleted in the heavy isotope. This results in each successive rainfall having an even lighter $\delta^{18}O$ value as the air mass migrates from its original source, as illustrated in Figure 9.

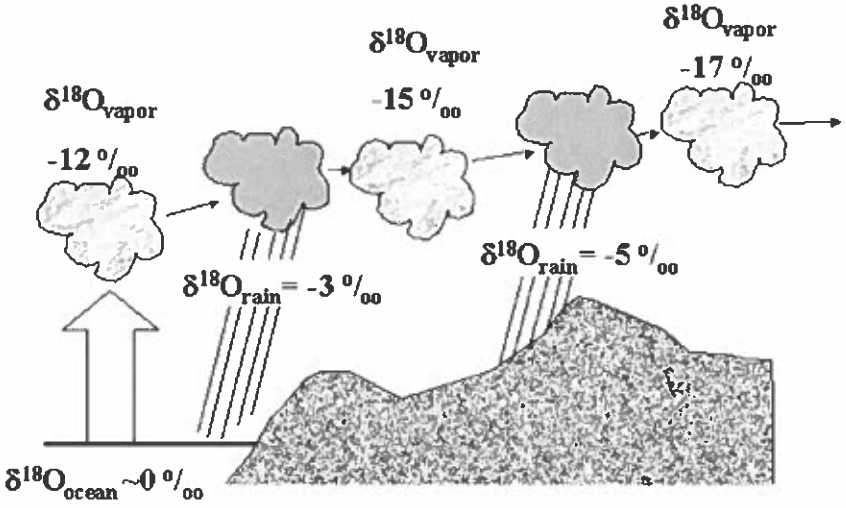

Figure 9. Rainout resulting from Rayleigh type distillations (from http://syllabus.syr.edu/GOL/disiegel/Gol400_600/isotopes.ppt)

5.5 Factors dictating the isotopic composition of precipitation

Numerous factors affect the isotopic composition of precipitation and influence the isotopic composition of the various sources of recharge waters. Perhaps the most important effect, related to this project, is the altitude effect due to the substantial topographic variations in the basin. Because temperatures drop with increasing elevation, precipitation becomes

isotopically lighter. Therefore, precipitation samples collected in mountain zone are more depleted in the heavy isotope than water condensing in the agricultural zone.

The altitude effect is essentially an incarnation of the temperature effect, which correlates isotopic composition with surface temperatures. This results from the temperature determining the amount of moisture in an air mass. Because most water is evaporated over the oceans, and the air masses migrate onto land, the temperature at which evaporation occurs is relatively steady for a given latitude. Therefore, the role of temperature in determining isotopic composition is principally in determining the fraction of vapor that will remain in the air mass.

The distance, or continentality effect, results from the Rayleigh-like processes governing the air mass. As the mass moves farther from the source, the precipitation becomes progressively lighter as a result of a greater number of precipitation cycles. As discussed above, each successive precipitation cycle results in the lighter water vapor, and thus isotopically lighter precipitation.

The seasonality effect is not overly relevant to the project due to the degree of mixing in the system being evaluated. The groundwater in this study is assumed to be well mixed and representative of the overall precipitation values for the given recharge sources. Essentially, the seasonality effect generally results in higher deuterium excesses in the winter versus the summer. However, the isotopic composition of seasonal precipitation in the Roswell Basin is likely controlled more by the source water of the air mass. The winter air masses are principally from the Pacific Ocean where surface temperatures are low. In contrast, summer precipitation originates in the Gulf of Mexico or the Gulf of California where surface temperatures area higher. A similar effect is observed in Albuquerque, NM (~200 miles north) as seen in Figure 10 (Sharp, 2002). The latitude and amount effects are not considered

here as a result of not being substantially relevant to the project as a result of little change in latitude in the basin and the time scale averaging that makes consideration of the amount effect unnecessary.

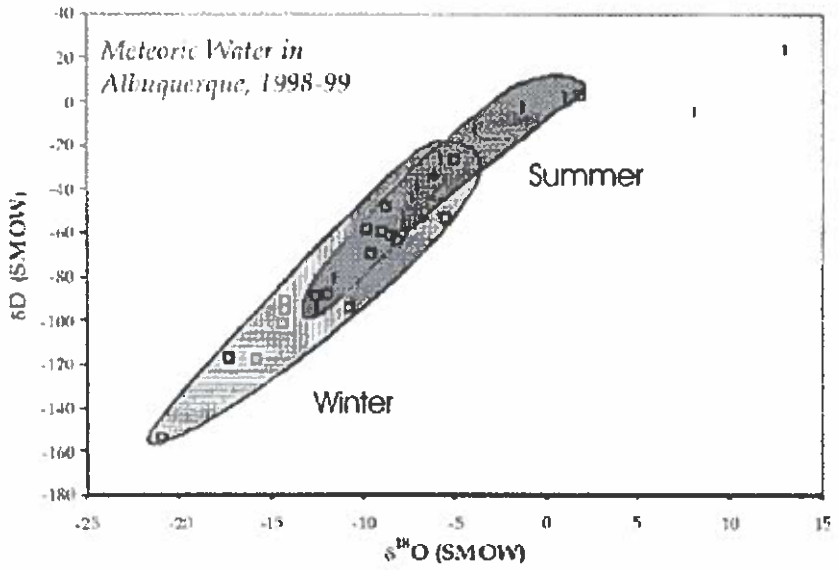

Figure 10. Seasonality effect as observed at Albuquerque, NM (Sharp, 2002)

5.6 Isotopic composition of precipitation in the Roswell Basin

Hoy and Gross (1982) collected precipitation samples for a one-year period at Roswell and Elk, NM. As a result of only collecting $\delta^{18}O$ data the validity of these data could not be evaluated, in that no δD versus $\delta^{18}O$ plot could be produced to determine whether much of these data also plotted above the GMWL. However, the weighted mean $\delta^{18}O$ values for the two sites were –6.0‰ and –7.1‰, respectively. From these values and the distance between the two sampling sites, Hoy and Gross calculated an altitude effect of only –0.18 ‰ / 328 ft., which is significantly less than –2.1‰ / 328 ft. that characterizes most of the world up to 16,404 ft. (Chamberlain et al., 1998).

Once recharge waters reach the saturated portion of the hydrologic system, they are generally treated as conservative tracers. While some isotopic exchange reactions between

water and evaporite bedrock were reported by Lambert (1978) in the Carlsbad, NM area, Hoy and Gross (1982) determined that no exchange reactions with the aquifer matrix have taken place in the Roswell Basin.

6.0 Isotopic analyses

6.1 Results

Fifty-four (54) samples were collected from various sources and analyzed in the stable isotope laboratory at the University of New Mexico. The results of these analyses are included as Appendix A and illustrated in Figure 11 (δD versus $\delta^{18}O$). Analysis of the data reveals that the $\delta^{18}O$ values of the data are very closely clustered between –7 and –8.5 ‰, with the exception of some surface waters.

Generally, the groundwater samples collected from the recharge area had the lowest $\delta^{18}O$ values, followed by the samples from the principal aquifer, with the samples from the alluvial aquifer having the highest $\delta^{18}O$ values. These results are logical because as groundwater migrates along flow paths they mix with water from faster recharge components. These faster recharge components typically have higher $\delta^{18}O$ values as a result of undergoing evaporation (secondary fractionations) or condensing at warmer temperature.

While there was a difference in the average $\delta^{18}O$ values from the recharge area and the principal aquifer area, it was very slight. Additionally, the spread of the data for each of the sources was wide ranging and values from each source overlap. The spread in the data amongst the sources is further evidenced by the large standard deviations in the data sets from each of the sources. While this was initially a cause for concern, it was determined that this overlap is a result of recharge mechanisms involved in the groundwater system. For example, the portions of the carbonate aquifer that receive a greater amount of recharge from underflow, would theoretically have lower $\delta^{18}O$ values because the source of the water in the

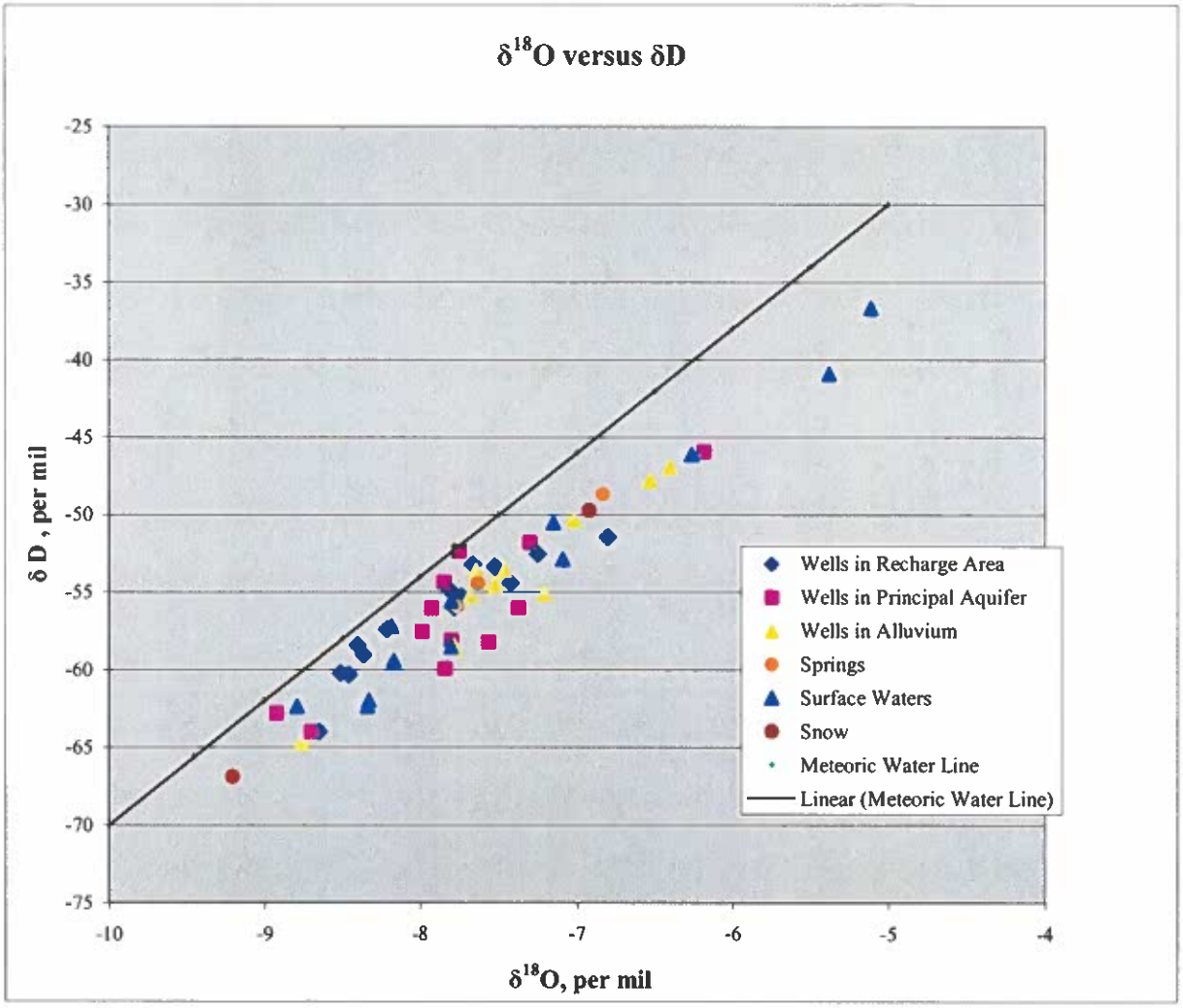

Figure 11. $\delta^{18}O$ versus δD

Table 3. Average isotopic values for various source areas

Source (# samples)	Average $\delta^{18}O$, ‰	Average $\delta^{18}D$, ‰	Median $\delta^{18}O$, ‰	Standard Deviation, $\delta^{18}O$
Wells in Recharge Area (14)	-7.90	-56.49	-7.80	0.55
Wells in the Principal Aquifer (12)	-7.76	-56.44	-7.82	0.69
Wells in the Alluvial Aquifer (11)	-7.44	-54.45	-7.52	0.65
Total Streams (12)	-7.40	-53.72	-7.80	1.2
"Recharge" Streams Only (9)	-7.93	-57.96	7.99	0.56
Springs (3)	-7.41	-53.04	-7.63	0.50
Snow (2)	-8.06	-58.32	-8.06	1.61

* All values reported with respect to SMOW

Yeso Formation condenses in the Sacramento Mountains and would have a lower $\delta^{18}O$ signature than water originating as precipitation in the agricultural zone.

Surface water samples vary from some of the isotopically lightest samples to the most enriched of any of the samples collected. Generally, those collected in the recharge area are isotopically light and those collected from the Pecos River are enriched in the heavy isotope. An enrichment in the heavy isotope along surface water flow paths is observed in samples from both the Rio Penasco and the Rio Puerco, as expected.

6.2 Comparison of results with previous investigators

Comparison of new data with those of Hoy and Gross (1982) provides several interesting results. Firstly, no statistically relevant changes in the $\delta^{18}O$ of water samples have occurred in the carbonate aquifer since the mid to late 1970's. For example, three of the samples collected in the principal aquifer became more enriched, while four others remained relatively constant. However, it is more likely this phenomenon is associated with seasonal variations in the aquifer hydraulics, rather than any long-term trend. Perhaps most importantly, a $\delta^{18}O$ versus δD plot of the "old' data and the new "data" (Figure 7) reveals that many of the "old" samples plot above the global meteoric water line, an extremely rare phenomenon. Therefore, either these samples were unique or portions of the analytical work were not properly conducted. As a result of these uncertainties, further comparison with these data was not pursued. However, it should be noted that the four samples that do plot below the GMWL are clustered with the newly collected data with $\delta^{18}O$ values between –7 and –8 ‰. Because much of the $\delta^{18}O$ is relative close to the new data, it may be that the problems were associated with the determination of the deuterium values.

7.0 Compartmental model theory

7.1 Fundamentals

A numerical compartmental or compartmental mixing cell model (Campana, 1975, Simpson et al., 1976, Campana and Simpson, 1984, Kirk and Campana, 1990) was used to simulate groundwater flow in the basin. The model was set-up by subdividing the basin into 20 mixing cells based on the spatial distribution of isotopic data and the subsurface geology. Each cell in the model represents a distinct region of the hydrogeological system, based on uniformity of the subsurface geology, determined principally by the work of Welder (1983) and $\delta^{18}O$ values. The compartmental model is a mass balance code that solves a more elaborate version of the continuity equation applied to a control volume:

$$dV/dt = I - O \qquad (1)$$

where dV/dt = time rate of change of volumetric storage in the system; and I and O are the volumetric inflow and outflow rates, respectively.

As a result of being unable to determine any significant transience in the $\delta^{18}O$ data (see section 6.2) the model was run using the steady-state simulation. In this case, I=O, and dV/dt = zero (cell volume is constant) and no information on storage properties can be obtained from the model; however information on groundwater flow paths, residence times distributions and recharge rates can be generated.

7.2 Tracer mass balance

The model simulates a mass balance equation for each individual cell as follows (Simpson, 1976):

$$S(N) = S(N-1)+[BRV(N)*BRC(N)]-[BDV(N)*BDC(N)] \quad (2)$$

Where: S(N) = the cell state at iteration N, the mass of tracer within the cell

BRV(N) = boundary recharge volume, the input volume of water at iteration N

BRC(N) = boundary recharge concentration, the input tracer concentration

BDV(N) = boundary discharge volume, the output volume of water leaving the cell

BDC(N) = boundary discharge concentration, the output tracer concentration

Recharge entering from outside the model boundaries is given a characteristic system boundary recharge concentration (SBRC), a characteristic system boundary recharge volume (SBRV), as well as system boundary discharge concentrations (SBDC) and a system boundary discharge volume (SBDV). During each iteration, equation (2) is applied to each cells discharge from bordering upstream cells are converted to recharge values for downgradient cells. It follows that the only unknown in equation (2) is the BDC(N), which can be determined by assuming a particular mixing rule, such as piston flow or perfect mixing. In this model the author has decided to use the modified mixing cell (MMC) based on the experiences of previous investigators (Campana, verbal communication). The MMC

mixing cell simulates pure piston flow (no dispersion) as the BRV→VOL and perfect mixing as BRV→ zero. The governing equation for the MMC is as follows (Campana et al., 2002):

$$BDC(N) = S(N-1)/VOL \qquad (3)$$

Where: VOL = volume of water in the cell

7.3 Age calculations

When the system boundary recharge values are held constant for each time-step of a simulation the calculation of mean age or residence time of the water in a cell is possible (Campana, 1975). For the MMC (the selected mixing cell rule used in this model the calculation is as follows:

$$AGE = \left[\frac{VOL}{BRV} * DELT\right] + \Sigma\left[FBRV_i * \overset{k}{\underset{i=1}{}} AGEFBRV_i\right]$$

where:

AGE = mean age of the water in the cell

DELT = real time between iterations

$FBRV_i$ = fraction of all incoming water to the cell BRV which is from cell i

$AGEFBRV_i$ = mean age of $FBRV_i$

k = number of upgradient cells which contribute water directly to the cell

8.0 Model development

8.1 Introduction

The model was developed in order improve understanding of groundwater flow and recharge mechanisms in the carbonate aquifer. The model includes a network of 20 mixing cells as illustrated on Figures 12 and 13. Four cells are located in the mountain zone where groundwater occurs predominantly in the Yeso Formation and flows eastwards into the very conductive unconfined regions of the San Andres Formation or continues downwards in the less transmissive Yeso Formation. Five cells are located in the unconfined region and ten cells are located in the confined regions of the carbonate aquifer. The number of cells in the confined zone is principally a function of having collected more data in this zone, rather than descretization based on heterogeneities in the subsurface.

8.2 Effective cell volumes

The effective volume of each cell was calculated as follows. The area of each cell was calculated using AutoCad software and a properly scaled drawing of the subdivided basin. The calculated area was multiplied by the thickness of the producing zone (Welder, 1983). The producing zone in the carbonate aquifer varies from approximately 75 ft thick in the north to 50 ft in the south. This zone represents the interval that has the greatest secondary permeability, resulting from the dissolution of enhanced features such as fractures and cavities. As a result, this zone has much higher transmissivities than the unaltered sections of the formation below, which transmit water only through primary porosity. The thickness of cells 1, 2, 8, and 9 where calculated using an estimated thickness of 1000 ft and an effective porosity of 0.02, a typical value for sandstones (Fetter,1994).

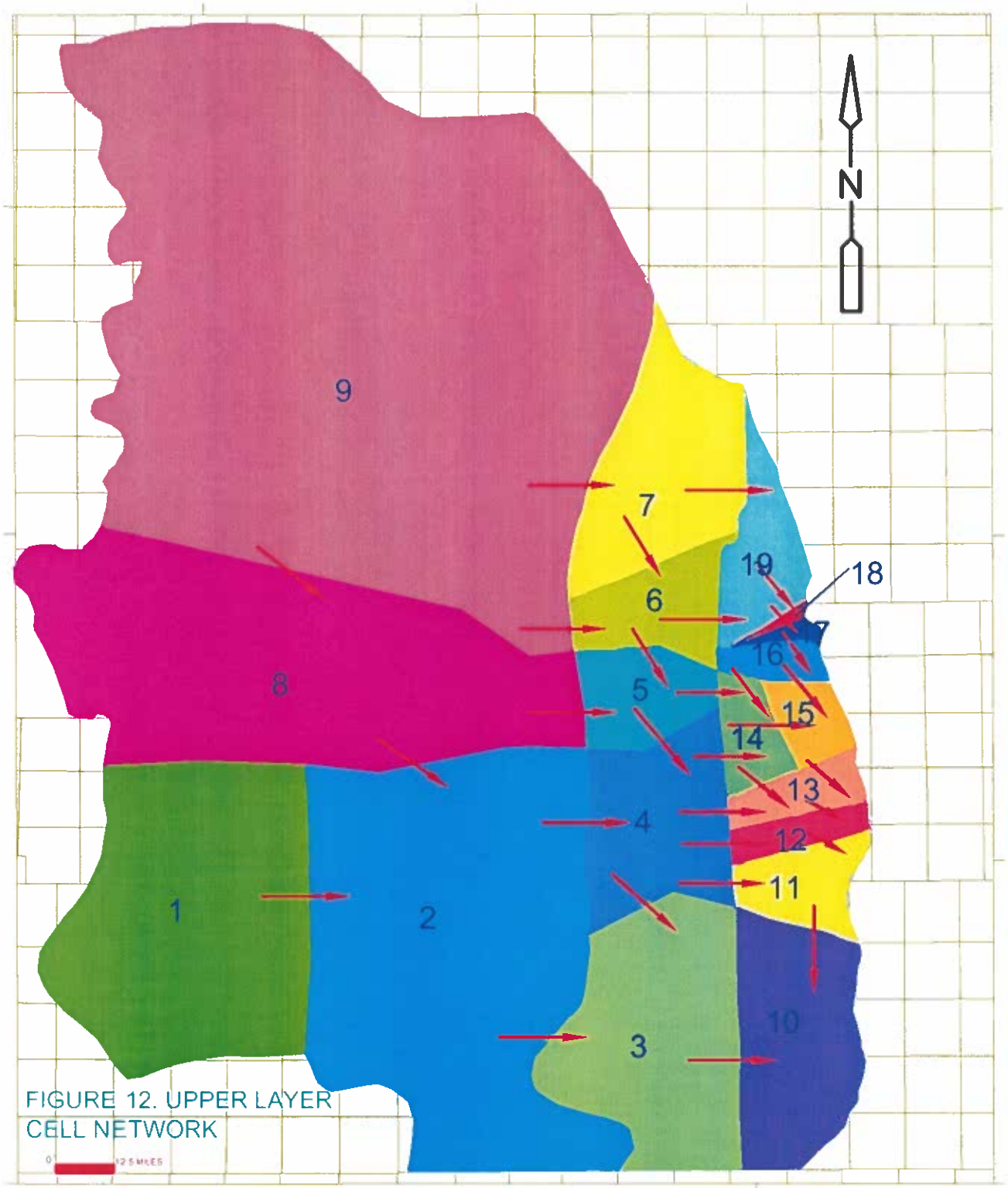

FIGURE 12. UPPER LAYER CELL NETWORK

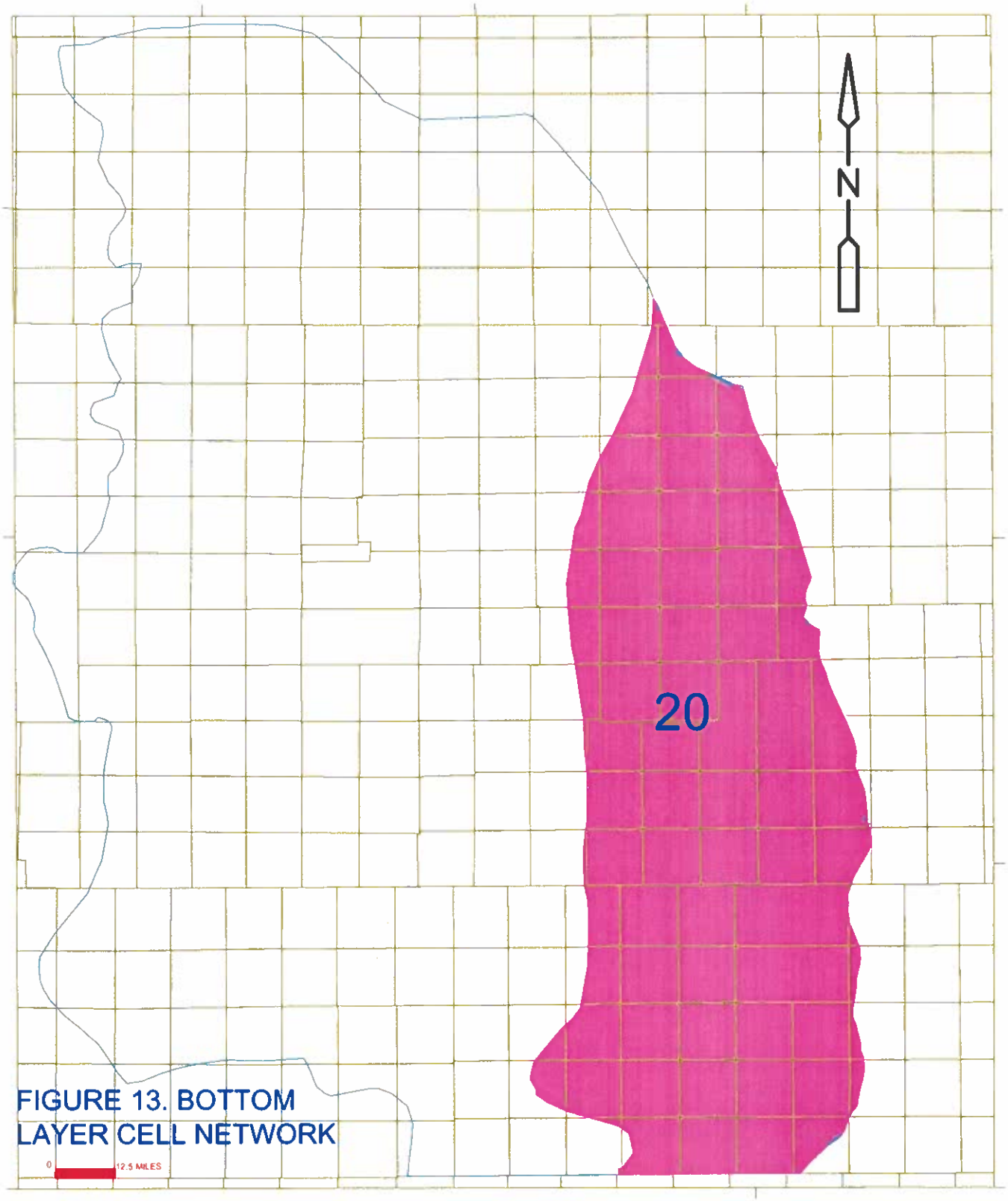

FIGURE 13. BOTTOM LAYER CELL NETWORK

Table 4. Effective cell volumes

Cell	Area ac	Thickness ft	Volume ac-ft	Effective Porosity	Effective Volume, ac-ft	Effective Volume, 100000 ac-ft
1	4.71E+05	1000	4.71E+08	0.02	9.42E+06	94.18
2	8.12E+05	1000	8.12E+08	0.02	1.62E+07	162.40
3	2.91E+05	50	1.45E+07	0.05	7.26E+05	7.26
4	1.69E+05	50	8.47E+06	0.05	4.24E+05	4.24
5	8.05E+04	75	6.04E+06	0.05	3.02E+05	3.02
6	8.77E+04	75	6.58E+06	0.05	3.29E+05	3.29
7	2.04E+05	75	1.53E+07	0.05	7.65E+05	7.65
8	6.42E+05	1000	6.42E+08	0.02	1.28E+07	128.39
9	1.79E+06	1000	1.79E+09	0.02	3.57E+07	357.00
10	1.91E+05	50	9.53E+06	0.05	4.77E+05	4.77
11	6.38E+04	75	4.78E+06	0.05	2.39E+05	2.39
12	3.13E+04	75	2.35E+06	0.05	1.17E+05	1.17
13	4.23E+04	75	3.18E+06	0.05	1.59E+05	1.59
14	4.42E+04	75	3.31E+06	0.05	1.66E+05	1.66
15	3.80E+04	75	2.85E+06	0.05	1.42E+05	1.42
16	2.61E+04	75	1.96E+06	0.05	9.79E+04	0.98
17	7.31E+03	75	5.48E+05	0.05	2.74E+04	0.27
18	4.62E+03	75	3.46E+05	0.05	1.73E+04	0.17
19	8.93E+04	75	6.70E+06	0.05	3.35E+05	3.35
20	1.37E+06	1200	1.64E+09	0.02	3.29E+07	328.74

8.3 Initial system boundary recharge conditions

Four components of recharge to the carbonate aquifer (or Yeso Formation in mountain zone) were incorporated into the model:

1. Tributary seepage
2. Direct infiltration of precipitation and irrigation return flow into areas where the top of the carbonate aquifer is not overlain by a confining unit
3. Underflow from the Glorieta Member and Yeso Formation
4. Lateral inflow from the Glorieta Member and Yeso Formation

The third and fourth processes listed are incorporated into the groundwater flow model and therefore are not considered system boundary recharge (SBR). The details of how these two mechanisms contribute to carbonate aquifer recharge are discussed in section 4.1.

The greatest contributor, other than underflow (which is simulated by flow in the model), is areal recharge (precipitation), which accounted for 16% or approximately 39,200 afy in the OSE model. The initial SBRV for areal recharge was calculated using the closest raingage for each cell and assuming that 5% of the precipitation eventually recharged the underlying carbonate aquifer. Table 5 shows what cells this SBR was applied to and the manner in which the SBRV was calculated for each cell.

Table 5. Estimates for areal recharge

Cell	Area ac	Precip. ft/yr	Station Name	Index Number[1]	Est. recharge to deep aquifer,%	Est. recharge ac-ft
1	4.71E+05	1.37	Elk	2865	0.05	32200
2	8.12E+05	1.37	Elk	2866	0.05	55500
3	2.91E+05	1.23	Hope	4112	0.05	17900
4	1.69E+05	1.37	Felix	3174	0.05	11600
5	8.05E+04	0.94	Hagerman	3792	0.05	3700
6	8.77E+04	1.18	Roswell FAA	7610	0.05	5200
7	2.04E+05	0.82	Roswell WB	7609	0.05	8300
8	6.42E+05	1.19	Picacho	6804	0.05	38200
9	1.79E+06	1.38	Capitan	1440	0.05	123100

[1] Number assigned to the station by the National Atmospheric and Oceanic Administration

The SBRC was estimated using the average $\delta^{18}O$ value of precipitation samples from Elk, NM (-7.1‰, recharge zone cells) and Roswell, NM (-6.0 ‰, agricultural zone cells) calculated by Hoy and Gross (1982). A value of 8.4 ‰ was assigned to precipitation in cells 1 and 9, to account for the altitude effect between Elk, NM and topographically higher locations within these cells. A slightly lower value of 7.7‰, an average of 8.4 ‰ and 7.1‰, was used in cell 8.

Another significant contributor to recharge of the carbonate aquifer is tributary seepage, which accounted for 10% or 24,500 afy of recharge to the carbonate aquifer in the OSE model. Tributary recharge to the carbonate aquifer occurs in the western portion of the where the San Andres Formation is under unconfined conditions where water flowing in streams flows through fractures and cavities into the formation. The SBRC for the source was estimated to be –7.9 ‰, the average of the stream samples collected in the recharge areas. However, tributary seepage also occurs in cells 1,2,8 and 9 where water infiltrates into the Glorieta Member and Yeso Formation. The SBRC for these cells was assigned based on the $\delta^{18}O$ value of the stream samples collected at the respective locations, with the exception of cell 9, where no samples were collected and an initial estimate of –8.5 ‰ was used.

The SBRV for tributary seepage to each cell was initially estimated using a total value of 24,500 afy as quantified by the OSE model. The distribution was estimated based on the work of previous investigators (Bean, 1949; Gross and Hoy, 1980; DBS&A, 1996) that identified the reaches of various tributaries to the Pecos River where channel infiltration is an important process. Generally, streams in the northern portion of the basin such as the Rio Hondo are believed to contribute greater volumes of water to the carbonate aquifer through channel infiltration then streams in the southern portion, such as the Rio Felix and Rio Penasco. For the purpose of this model both the SBRV and SBRC were assumed to be constant throughout the entire period of simulation.

8.4 Additional initial conditions

A time step of one year was used as a result of most of the input data sources providing yearly values of recharge, discharge etc. The period of simulation is 1401 years, from 600 to the year that the samples were collected, 2001. Initially the model was simulated

using a period of simulation from 1900 to 2001, to simulate the onset of groundwater pumping in the basin. However, using this period of simulation very few of the cells reached steady-state with respect to $\delta\ ^{18}O$ values during the simulation due to the long flow paths and residence times in the subsurface.

The model assumes that the initial groundwater in the year 600 is similar to that of the precipitation in the Sacramento Mountains, or –8.5 ‰. The initial estimates of intercell flow distributions where accomplished using hydraulic head gradients in the carbonate aquifer, as reported by DBS&A (1996) for the year 1984.

The model requires that a discharge be associated with each cell and that the sum of the total intercellular flow and the discharge be equal to one cell volume. The initial discharge rates were nominally estimated from the discharge inputs from the OSE model. However, because discharge in the model incorporates discharge by springs, upward leakage to the alluvial aquifer and groundwater pumping, many of the cells on eastern margin of the model discharge all of the inflow for a given iteration.

9.0 Results of the model

9.1 Calibration results

The goal of the modeling effort was to achieve a calibrated $\delta^{18}O$ for each cell that was within 0.1‰ of the target $\delta^{18}O$ value. This was accomplished in 13 of the 20 cells with target $\delta^{18}O$ values (Table 6) by adjusting the intercellular flow paths and to a lesser extent the flux boundary conditions until calibration was achieved. The remaining cells were calibrated to within 0.5 ‰ of the target $\delta^{18}O$ values, with the exception of cell 12 which is off by 1.2 ‰.

Table 6. Calibration results

Cell	Target $\delta^{18}O$	Calibrated $\delta^{18}O$	Difference
1	-8.5	-8.5	0.0
2	-8.0	-8.0	0.0
3	-7.5	-7.5	0.0
4	-7.2	-7.2	0.0
5	-7.7	-7.7	0.0
6	-7.8	-7.7	-0.1
7	-8.5	-8.2	-0.3
8	-7.4	-7.4	0.0
9	-8.5	-8.4	-0.1
10	-8.0	-7.8	-0.2
11	-7.3	-7.3	0.0
12	-6.3	-7.5	1.2
13	-7.8	-7.8	0.0
14	-7.9	-7.8	-0.1
15	-7.4	-7.8	0.4
16	-7.6	-7.7	0.1
17	-8.7	-8.2	-0.5
18	-7.8	-8.2	0.4
19	-8.5	-8.2	-0.4
20	-8.2	-8.2	0.0

The target $\delta^{18}O$ value of –6.18 ‰ in cell 12 is not achievable as there is no mechanism in the model to reach such a high $\delta^{18}O$ value. It seems likely that this well is heavily influenced by downward leaking waters from the alluvial aquifer resulting from gradient reversals caused by heavy groundwater pumping. This process is further supported by a $\delta^{18}O$

value increase of more than one permil since Hoy and Gross (1982) sampled the same well in 1978. The volume of water leaking from the alluvial aquifer should increase over time as continued aquifer pumping will continue to decrease the potentiometric surface in the carbonate aquifer resulting in more extensive leakage. However, since the alluvial system is not considered in the model this could not be modeled appropriately.

In contrast, several cells could not reach complete calibration due to the lack of a mechanism to reach such low $\delta^{18}O$ values. This was true in cells 7,17, 19 were the cells were -8.4 permil or lighter and the lightest SBRC in the model was -8.5 permil. When mixing SBR's with lower concentrations is considered, it is impossible to reach the values of -8.4 and lower. This condition is quite troubling as it indicates that waters with values lower than -8.5 permil play a role in recharging the carbonate aquifer. It may be that the Glorieta Member and Yeso Formation should not be lumped into a single cell beneath the San Andres Formation. In this scenario the flow from cells 2, 8 and 9 into the Yeso Formation are thoroughly mixed. It may be that a model that describes the Yeso Formation in three cells would be more accurate. This would allow for water in the northern portion of the Yeso Formation to reflect the isotopic composition of the water flowing into the formation from cell 9, which is considerably lighter than the $\delta^{18}O$ value of the modeled Yeso underflow as a whole.

All of the cells in the model reach a steady-state $\delta^{18}O$ value within the period of simulation (Appendix B). It was anticipated that the cells near recharge areas would reach steady-state quite rapidly, and that the easternmost cells would take considerably longer as a result of long flow paths in the subsurface. However, this was not the case. Nearly all of the cells reach a steady-state at approximately 1000 years (except with cell 1 and 9, whose steady-state values are very close to the initial state). Early changes in concentration are

observed in the first hundred years, as a result of the "fast" recharge components. The second slope for many cells is a manifestation of the "slow" recharge components, in this case, Yeso underflow.

9.2 Groundwater flow and recharge estimates

The model provides some insight into the flow of groundwater, not characterized by previous investigators. The total recharge estimates agree well with previous estimates as seen in Table 7.

Table 7. Comparisons of recharge estimates for the carbonate aquifer

Source	Lateral Inflow	Yeso Form. Underflow	Tributary Seepage	Areal Recharge	Total Recharge to Carbonate Aquifer
DCMC Model	**70,200**	**92,400**	**34,200**	**34,100**	**230,900**
DBS&A, 1996	58,000	181,100[2]	24,500	39,200	245,000
Summers, 1972					231,900
Hantush, 1957					257,000

* the units of volumes in the above table are acre-feet/year

[1] These values were adjusted to include only the recharge over the unconfined/confined zones of the model to allow for comparison with previous investigators.

[2] lateral inflow is included as Yeso underflow in the DBS&A MODFLOW model, but estimated it based on the hydraulic gradient, transmissivity, and the length of the contact

The total recharge and the total volume of recharge emanating from the Glorieta Member and Yeso Formation are very comparable to the conclusions of the OSE model. However, the amount of lateral inflow is considerably higher, particularly through cell 8 were the inflow was 1900 afy/mile. This inflow would require a transmissivity of approximately 270,000 ft^2/d (calculation follows assumptions listed in DBS&A, 1996). This is substantially higher than the 90,000 ft^2/d estimated by the DBS&A (1996) for the average transmissivity along the contact. Cell 8 is separated from the highest transmissivity zone in the entire OSE model in the San Andres Formation of 300,000 ft^2/d by a narrow zone with a transmissivity of 100,000 ft^2/d. Therefore, the OSE model may underestimate the transmissivity of the Yeso

Formation in this area, in which case the same processes, which have increased the transmissivity of the San Andres Formation in the area, may also have done the same for the Yeso Formation , which has extensive evaporite sequences in the northern portion of the basin (Bean, 1949). The calculated transmissivities for cell 2 and 9 are nearly an order of magnitude lower so the overall transmissivity of 90,000 ft^2/d remains reasonable.

As seen in Table 8, the calibrated recharge values for tributary seepage are considerably higher than in the OSE model. The greatest amount of channel infiltration occurs along the Rio Hondo, as expected. There is also a large volume of seepage occurring in the southern portion of the basin along the Rio Penasco and the Rio Felix, where little seepage was thought to be occurring. The values predicted by the compartmental model are approximately three times that calculated with the OSE model along these reaches.

Table 8. Calibrated system boundary recharge volumes

Recharge Source	cell 1	2	3	4	5	6	7	8	9
Areal	21000	10300	12900	10100	3000	7100	1000	19100	49950
Tributary Seepage	7500	14400	9000	6500	9500	8600	600	21250	20000
Total SBRV	28500	24700	21900	16600	12500	15700	1600	40350	69950

* all values reported are in acre-feet/year (afy)

However, previous investigators such as Bean (1949) calculated estimates consistent with the model for seepage along the Rio Penasco, based on stream gauge measurements.

The cells receiving the greatest amount of recharge from underflow are 10, 14, 5, 6, 13, 7 and 19 (see Table 9). Large structural features pass through each of these cells (except cell 13), suggesting that these faults are providing the necessary conduit for waters to be rapidly transmitted upward as initially hypothesized by Wasiolek (1981). The model also confirms the concept that the bulk of underflow occurs in the northern half of the basin, with the exception of cell 10. Previous investigators (DBS&A, 1996) have concluded that no

Table 9. Calibrated flow distribution

Discharging Cell	Receiving Cell	Flow Fraction	Discharging Cell	Receiving Cell	Flow Fraction
9	8	0.010	20	19	0.053
9	7	0.150	7	6	0.020
9	6	0.080	7	19	0.980
9	20	0.760	6	5	0.670
8	1	0.020	6	19	0.090
8	5	0.520	6	16	0.110
8	2	0.250	5	4	0.002
8	20	0.200	5	14	0.768
1	2	0.990	4	3	0.020
2	3	0.340	4	11	0.540
2	4	0.080	4	12	0.275
2	20	0.580	4	13	0.055
20	3	0.050	4	14	0.000
20	4	0.030	3	10	0.500
20	5	0.140	19	18	0.040
20	6	0.107	18	17	0.010
20	7	0.080	17	16	0.002
20	10	0.258	16	14	0.090
20	11	0.019	16	15	0.005
20	12	0.000	14	15	0.030
20	13	0.085	14	13	0.700
20	14	0.125	15	13	0.150
20	15	0.000	13	12	0.100
20	16	0.001	12	11	0.010
20	17	0.040	11	10	0.050
20	18	0.000			

upward leakage occurs east of the K-M structural zone and that very little underflow occurs in the southern portion of the basin. However cell 10 (southernmost cell), which the K-M structural zone runs through, received significant underflow. It may be that the K-M structural zone provided the necessary conduit for recharge after which the water continued to flow southeast to the sample location (as predicted by the hydraulic gradient). It is not possible to know for sure as a result of the structural zone passing through the cell in question.

It is interesting to note that the initial isotope data for cells receiving significant Yeso underflow also had much lower deuterium excess parameters. For example, the five cells that

receive the most underflow in the confined zone, 10, 13, 14, 17 and 19, have an average deuterium excess of 3.01 per mil. In contrast, the five other cells in confined zone of the carbonate aquifer had a deuterium excess of 6.01 per mil. This further supports the conclusion that water with a source in the Sacramento Mountains that would be expected to have a lower deuterium excess parameter, is recharging these cells. The lower deuterium excess is due to the smaller moisture deficits in the mountain climate. In contrast, in cells where recharge is principally in the form of diffuse recharge, the deuterium excess parameter is greater as a result of greater moisture deficits in the more arid climate of the agricultural zone. Therefore, the lower deuterium excess in the cells receiving recharge waters from Yeso underflow in the model provides further supports for this hypothesis.

9.3 Mean groundwater ages

The minimum mean groundwater ages in the system range from 243 years to 924 years old (Figure 14). As expected the youngest waters occur in the recharge area cells; however, the groundwater ages of cells in unconfined and confined portions of the carbonate aquifer are mixed. That is to say that the mean age of groundwater in an unconfined zone cell can be older than that of a confined zone cell if the mass balance is such that the cell receives much more recharge from upward leakage than tributary seepage and diffuse recharge. Therefore, groundwater age is principally controlled by how much recharge a cell is receiving from the Yeso underflow. Recharge to the upper layer cells from the Yeso Formation is old, as a result of the long flow paths and residence times in cell 20. This water mixes with younger recharge waters to the cell such as flow from another cell in layer 1 or from tributary seepage to achieve a final cell state.

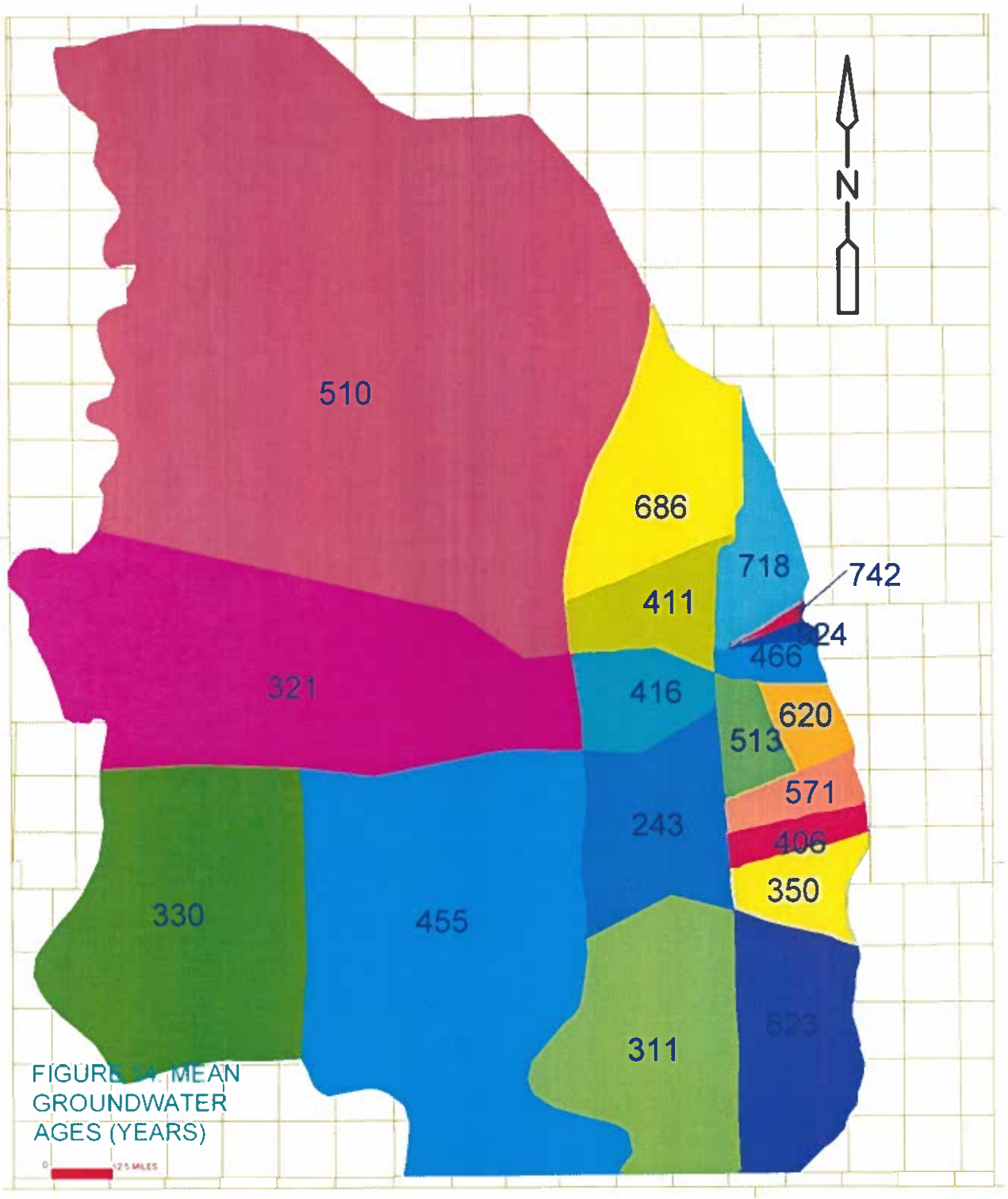

FIGURE 14. MEAN GROUNDWATER AGES (YEARS)

9.4 Sensitivity analysis

A sensitivity analysis was conducted in order to determine how a miscalculation of a modeled parameter would affect the model output. Sensitivity analysis of the mixing cell model is unusually in that modeled parameter (flow distribution) is the independent variable and the dependent variable is the tracer concentration during the final iteration of the model. The most pragmatic way to test for sensitivity is to vary the independent input variables such as recharge volume and concentration, initial state, flow distribution and cell effective volume. Three cells were chosen to for sensitivity analysis: cells 4, 8, and 11. Cell 8 was selected to represent a cell in the recharge area, cell 4 represents a cell in the unconfined zone and cell 11 represents a cell in the confined zone.

9.4.1 System boundary recharge volume

The system boundary recharge volumes for both tributary seepage and areal recharge were varied by ±50%. The change in SBRV was distributed to all of the SBR cells in a weighted fashion with each specific SBRV being increased and decreased by 50%. These changes resulted in relatively small changes in the $\delta^{18}O$ value of the cells at the final iteration (Figure 15 and Figure 16). The effects varied from less than 0.1‰ to greater than 0.2‰ for both types of SBR. Given that the analytical error associated with the analyses was 0.1‰, this was a troubling result. This analysis indicates that relatively large errors associated with estimating the SBR would result in relatively small effects on final cell conditions.

9.4.2 System boundary recharge concentration

The SBRC or $\delta^{18}O$ value for each of the two sources of recharge was varied by ±50% to evaluate the sensitivity of this parameter. As expected the change resulted in significant changes in the cells state at the final iteration. As displayed graphically on Figure 17 and Figure 18, the SBRC changes resulted in final conditions that were ±2 ‰ from the final conditions of the model results. This indicates the model is quite sensitive to this parameter and small errors in the assumptions and measurements of the SBC for both tributary seepage and areal recharge could affect the model output significantly.

9.4.3 Effective cell volumes

The effective cell volume was varied by ±50%. The effects of changes in cell volume resulted in relatively minor changes in cell states. Only cell 8 was affected significantly in terms of the final $\delta^{18}O$ value, which varied by 0.1‰ to 0.15‰. This is not so surprising and may be a result of not reaching steady-state conditions because of the substantially greater or lesser volumes of water being stored in the cell. This would also explain why cell 8 was affected the greatest, as it stores the most water of the three cells. As seen in Figure 19, changes in the cell volume substantially altered the calculated groundwater ages. Changes in the groundwater ages varied from a difference of 100 years to a difference of greater than 200 years.

9.4.4 Initial state

The initial state of the selected cells was varied by ±50%. Surprisingly, this resulted in

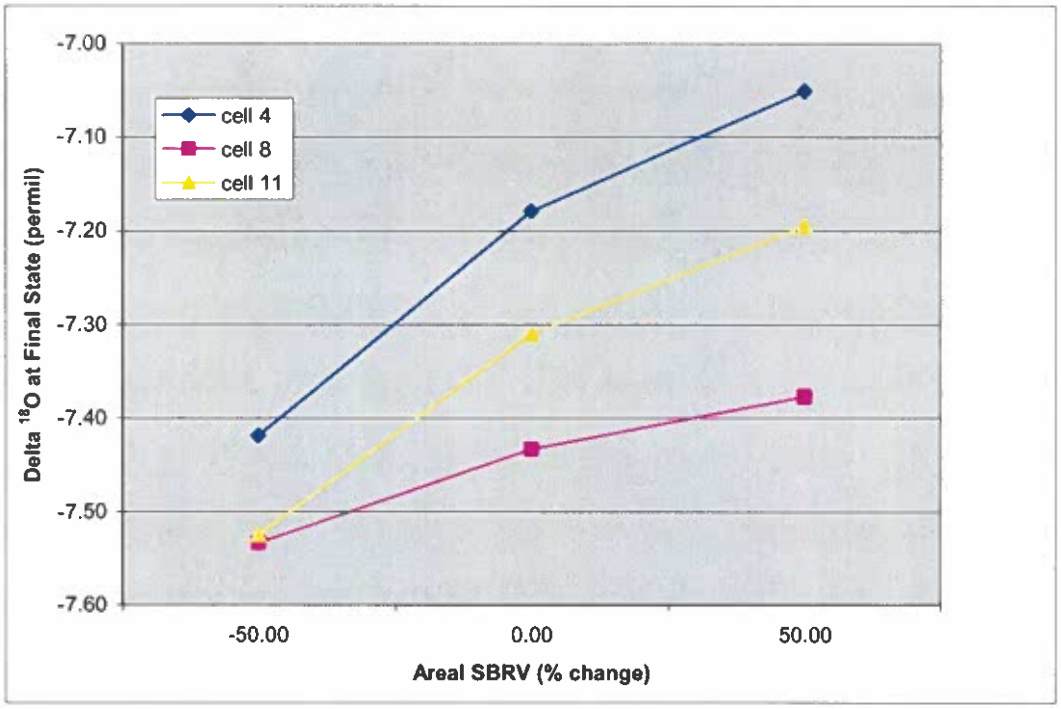

Figure 15. Sensitivity plot for areal SBRV

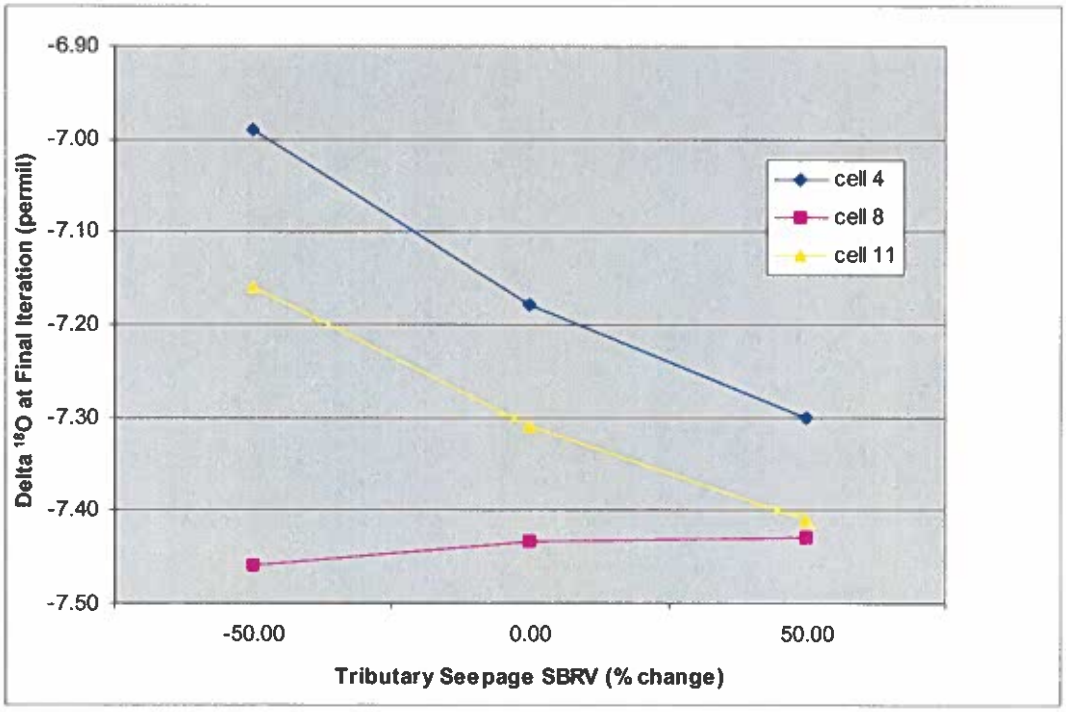

Figure 16. Sensitivity plot for tributary seepage SBRV

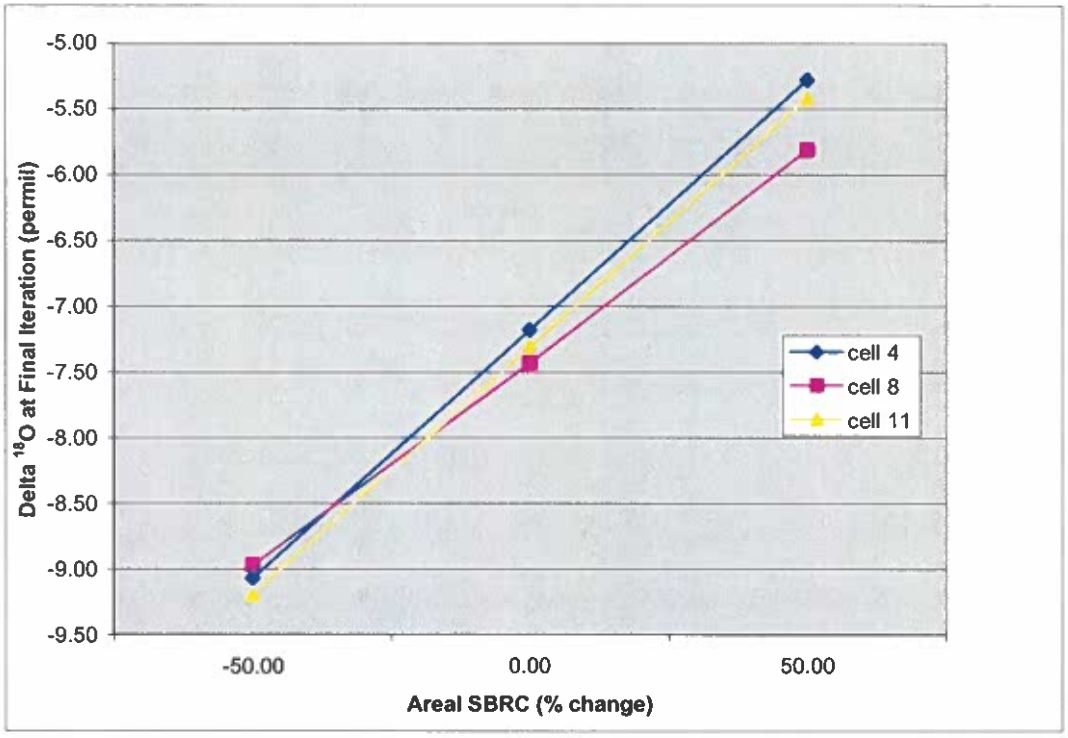

Figure 17. Sensitivity plot for areal SBRC

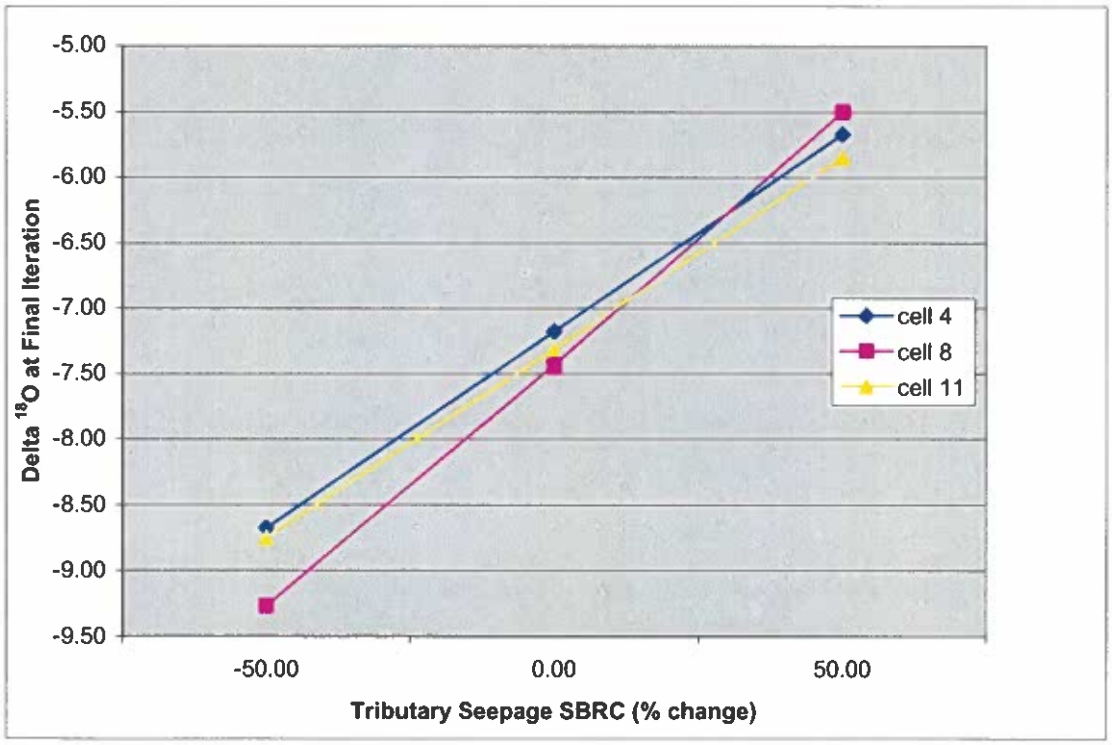

Figure 18. Sensitivity plot for tributary seepage SBRC

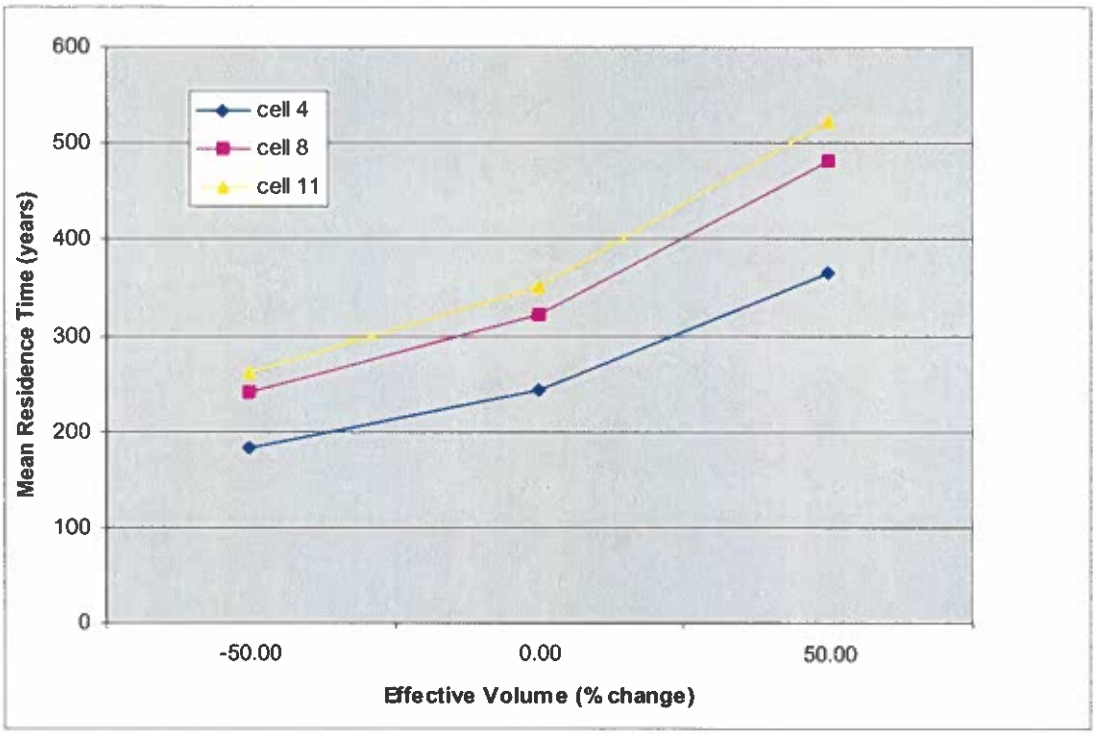

Figure 19. Sensitivity plot for effective cell volume

significant changes in the cell states at the final iteration. As seen in Figure 20, the final cell states were affected by nearly 2‰. The changes amounted to greater than 4‰, which is significant. However, these cells did not reach steady-state conditions during the simulated period. There is confidence that if the simulation period were extended that the cell states would be nearly, if not identical, to the current cell states at the final iteration of the model.

9.4.5 Flow fraction of contributing cell

Three pairs of cells (8 to 5, 3 to 10, 20 to 14) were selected to analyze the sensitivity of the model to variations in the groundwater flow paths. The first pair was selected to simulate flow from a recharge zone cell to an unconfined zone cell. The second pair represents flow from an unconfined zone cell to a confined zone cell and the third pair was

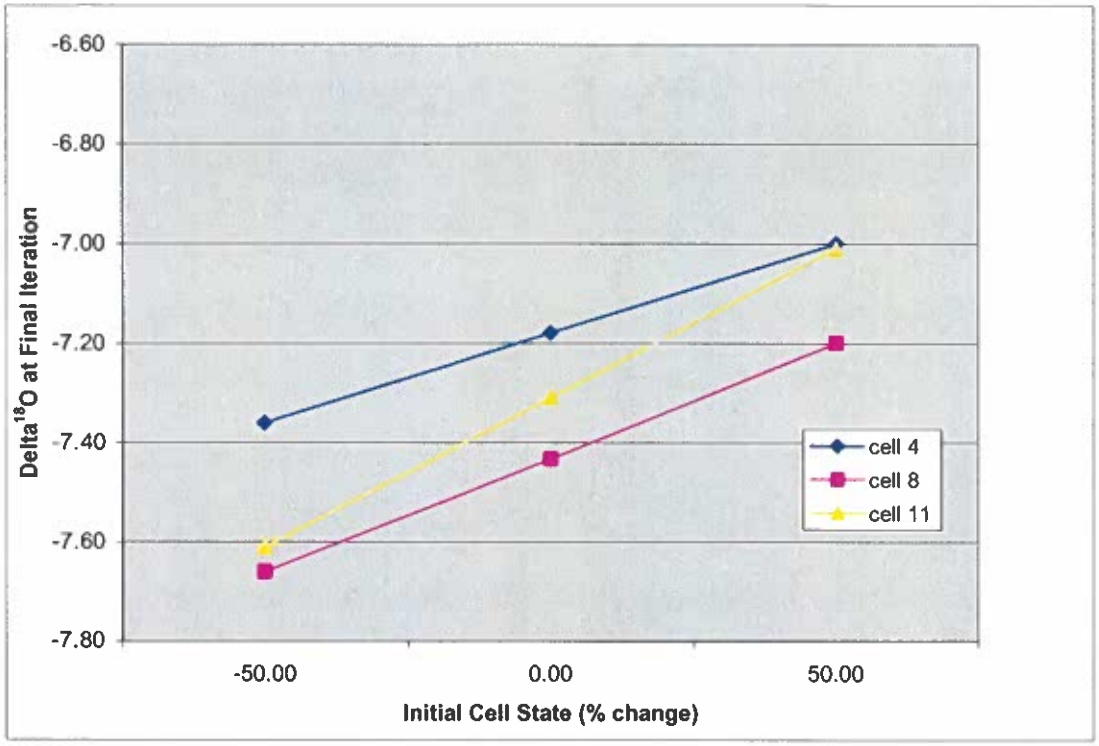

Figure 20. Sensitivity plot for initial cell state

chosen to represent a cell that receives significant underflow from cell 20. Figure 21 illustrates the results on the receiving cell of altering the fraction of flow from the contributing to the receiving cell by ±50%. The figure illustrates the relatively low sensitivity of the model to changes in the amount of flow being distributed to receiving cells. This is a concern, as a central goal of the modeling effort was discern groundwater flow paths in the basin.

Even though most cells were calibrated to within the analytical error of the isotope analyses, the model may not correctly represent actual conditions in the subsurface as a result of the low sensitivity to flow distributions. However, it should be noted that the author has significant confidence in the ability of the model to reasonably simulate upward leakage of from the Yeso Formation. This is a result of the substantial changes in isotopic composition along some of the flow paths. The lateral flow paths in the model agree well with the

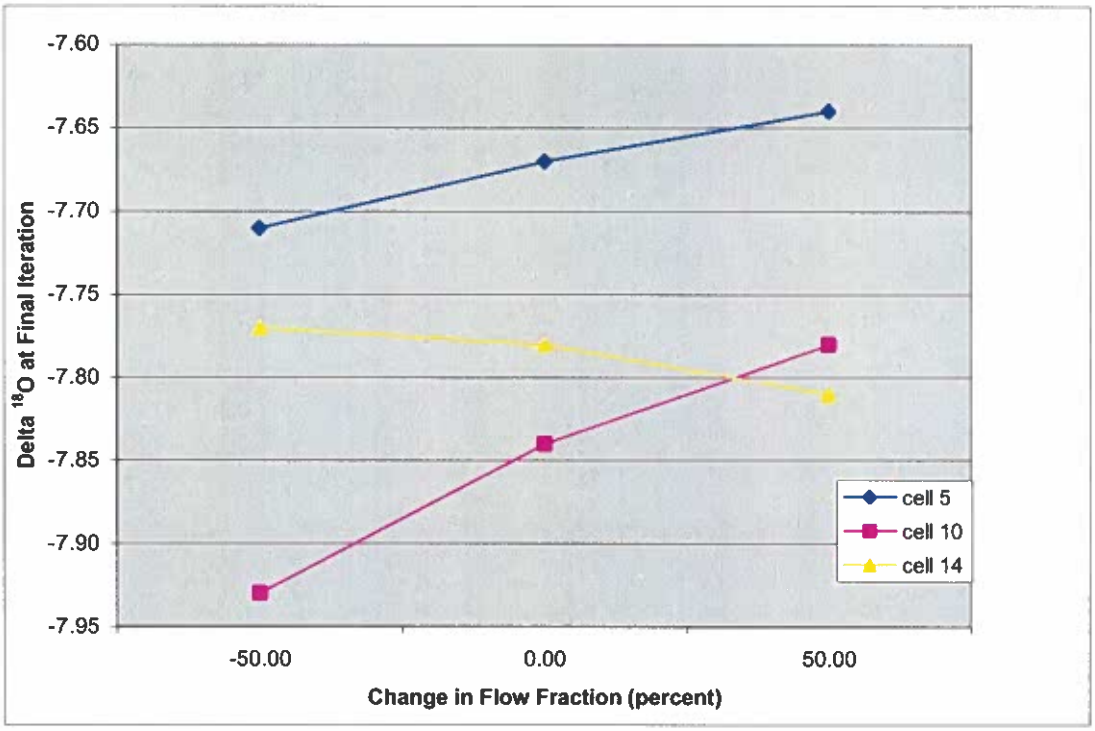

Figure 21. Sensitivity plot for changes in the flow fraction from the contributing cell to receiving cell

hydraulic gradient data (DBS&A, 1996) and the OSE model, which further enhances the author's confidence in the model.

10.0 Summary and conclusions

The data suggest that the $\delta^{18}O$ values of waters in the basin have remained relatively constant since the 1970's. The exceptions are several wells in the southeastern portion of the basin where downward leakage of water from the alluvial aquifer through the Artesia Formation is likely raising $\delta^{18}O$ values.

In general the results of the compartmental model are in agreement with the OSE model. The model predicts an overall recharge to the carbonate aquifer of 230,900 afy, 6% less than the OSE model. The results also suggest that recharge from Yeso underflow is the dominant recharge mechanism for the carbonate aquifer. Most of the upward leakage occurs in the northern portion of the basin and is likely transmitted through structural features that have enhanced secondary permeability as a result of fractures and subsequent dissolution of the carbonate rock as a result of the increased flow. However, some upward leakage does appear to be occurring the southeastern most section of the basin, a phenomenon not previously thought to be occurring. The model predicts significantly more lateral inflow than previously thought, particularly in the north central portion of the basin. This may be indicative of high transmissivity values for the Yeso Formation (or Glorieta Member of the San Andres Formation) in this area, which would coincide with the very high transmissivities determined for carbonate aquifer just east of the contact by previous investigators (Rehfeldt and Gross, 1982; DBS&A, 1996). Lastly, the model predicts greater channel infiltration recharge (than the OSE model) in the southern portion of the basin, consistent with previous field investigations (Bean, 1949).

While not mathematically well constrained the model is still a valid tool in assessing groundwater flow in the basin. However, for the same reason future efforts may want to focus on using alternative subsurface tracers.

11.0 Recommendations for future work

Any future work with a similar focus should concentrate on establishing more accurate SBRC's, to increase model accuracy. A larger number of samples from all areas would be very beneficial in that it would allow for greater descretization and likely more accurate modeling results. Incorporating an additional layer to simulate flow paths in the alluvium would allow for downward leakage to be incorporated into the model. Additionally, the Yeso Formation underneath the San Andres Formation should modeled as more than one cell. However, it may not be possible to obtain samples from wells screened only in the Glorieta Member and Yeso Formation in the eastern portion of the basin, which would make this difficult. The collection of samples in the structure zones and comparing these samples with ones farther away from these zones where waters are likely more mixed could confirm the role of these structures in the recharge dynamics of the basin. However, as a result of the homogeneity in the stable isotope data the author suggests that mixing cell models calibrated with other geochemical tracers may prove more fruitful in discerning groundwater flow in the basin.

Appendix A. Analytical results

Appendix A. Sampling results from Hoy and Gross (1982) and this study

Sample ID	Location	Date Collected	Delta ^{18}O ‰	Delta D ‰	GPS	Notes
Wells screened in the Carbonate Aquifer						
WP-1	10.25.22.324	March-75	-8.80	-52.0		
		November-78	-7.60	-50.1		
WP-MG-1	Near original WP-1	August-01	-7.80	-58.1	N33°23.646', W104°28.741'	Chase Farms, Donald 505-624-9310, 900 gpm
WP-2	RWTP	June-76	-7.70	-52.5		
	RWTP	March-01	-7.92	-56.1		
WP-MG-2		August-01	-7.56	-58.2	N33°18.505', W104°28.702'	Farm 5 mi. South of Roswell (same property as WA-MG-2)
WP-4	Clardy Irrigation Well	August-02	-8.70	-64.0		
WP-8		August-01	-7.37	-56.1	N33°13.167', W104°19.792'	Glen Marshall, 734-5810 sample from deep well
WP-9	Villa Solano	April-78	-7.20	-31.1		
	Villa Solano	December-78	-7.70	-52.7		
	Villa Solano	March-01	-7.85	-54.4		Now the Roswell Correctional Facility
WP-10	Hagerman Municipal Well	April-78	-7.40	-56.9		
		December-78	-7.80	-54.1		
		March-01	-7.75	-52.4		Hagerman city well, sample at fire department
		August-01	-7.84	-60.0	N33°06.851', W104°19.539'	
WP-11	Jake Johnson Farm	December-78	-7.70	-58.5		
		March-01	-6.18	-45.9		W on Fox Rd. 5 mi S of Hagerman, 90 W for 1 mile
WP-12	Pollard Well	September-77	-9.40	-51.0		old Pollard property, turn left on Anita off 2S and follow to end
		April-78	-9.00	-55.0		well not pumping much, sample from storage tank (evap likely)
		March-01	-7.30	-51.8		
WP-17	Vandiver Well	August-77	-9.20	-48.0		
	18.26.18.41124	April-78	-8.40	-50.3		
		August-01	-7.98	-57.6		
WP-MG-3	Berrendo Water Supply	August-02	-8.92	62.8	N33°23.663,104°33.513	Sample from home owner at GPS location at old WA-2 location
Wells in the Recharge Zone						
WR-3	Woods Well	December-77	-9.40	-46.7		
	11.22.09.321	June-78	-8.90	-41.8		
		March-01	-7.81	-54.9		Now Keith Schrimisker (take two rivers dam exit)
WR-5	Patterson Irrigation	June-78	-9.30			
		March-01	-7.78	-56.0		Now Calder Ezzel, house well in 73 is now irrigation well
WR-5B	Patterson domestic	June-78	-9.20			
		March-01	-7.66	-53.3		
WR-14	Hope Municipal	May-77	-7.20	-47.3		
		January-78	-7.20	-46.8		
		March-01	-7.74	-55.3		
		August-01	-7.25	-52.5		
WR-16		August-01	-6.8	-51.5		
WR-18		August-01	-8.36	-59.1		
WR-19	R.O. Anderson well	June-78	-9.30			
	11.18.15.313	March-01	-7.42	-54.5		
WR-MG-1		August-01	-8.21	-57.4		
WR-MG-2		August-01	-8.40	-58.4		
PVCD-2		August-01	-8.46	-60.3		

Appendix A. Sampling results from Hoy and Gross (1982) and this study

Sample ID	Location	Date Collected	Delta ^{18}O ‰	Delta D ‰	GPS	Notes
PVDC-3		August-01	-8.51	-60.2		
M-13	16.20.16.241	April-78	-7.20			
		March-01	-7.52	-53.4		located 5 mi north of HW13 near road
M-14	16.20.16.241	April-78	-7.80	-62.1		
		July-78	-8.10	-72.8		
		August-01	-8.65	-64.0	N32°54.953', W105°20.296'	Windmill at Elk, now well is a domestic well at Copper Ranch
Wells in the Alluvium						
WA-1		August-01	-7.68	-55.2	N33°23.663',W104°33.783'	Sampled replacement well for WA-1 (1/4 mi S), R.Jenkins
WA-MG-1	Chase Farms	August-01	-7.21	-55.1	N33°23.443, W104°28.469	600 gpm
WA-2		August-01	-7.46	-53.6	N33°23.663',W104°.33.543'	
WA-MG-2		August-01	-7.78	-58.4	N33°18.451', W104°28.657'	Farm located 5 mi south of Roswell, W of HW285
WA-6		August-01	-6.53	-47.8		
WA-7		August-01	-7.02	-50.3		
WA-9		August-01	-8.77	-64.8	N32°52.313',W104°24.690'	Tracy Kennebruck, shallow well (<200'), elev.3446'
WA-10	Gates RA 1331	August-75	-6.10			
	17.26.20.333	June-76	-7.70			
		August-76	-7.00			
		March-77	-5.40			
		July-77	-7.60			
		September-77	-7.60			
		April-78	-8.60			
WA-10B		March-01	-7.64	-53.6		Halderman water, located 1 mi east of original WA-10, well
		August-01	-7.52	-54.6	N32°50.579', W104°21.501	drilled to 210 feet, located about 1 mi. east of orig. WA-10
WA-11	D. Menefee well	July-77	-7.20	-51.1		
	17.26.30.211	April-78	-7.00	-55.5		
		August-01	-7.79	-58.6		Sample collected on E side of road, previously collected on S side
WA-12		August-01	-6.40	-46.9		
WA-MG1		August-02	-7.21	-55.1		
WA-MG2		August-02	-7.78	-58.4		
Springs						
F1		March-01	-7.76	-56.0		
F1B		March-01	-6.83	-48.7		
F2		March-01	-7.63	-54.5		
Surface Water						
S-4	Rio Bonito	June-78	-8.90			Rio Bonito at Baca Campground
		November-78	-10.10	-60.0		
		March-01	-7.09	-52.9		Sample at milepost 91, 1.5 miles past Fort Stanton exit
S-8	Rio Hondo at the	June-78	-7.30			
	R.O. Anderson well	December-78	-10.10			
		March-01	-7.15	-50.5		
S-10	Pecos River at Roswell	April-78	-12.6			
		March-01	-5.11	-36.7		
		August-01	-6.26	-46.1		

Appendix A. Sampling results from Hoy and Gross (1982) and this study

Sample ID	Location	Date Collected	Delta ^{18}O ‰	Delta D ‰	GPS	Notes
S-13	Pecos River at Artesia	April-78	-5.50			
		March-01	**-5.38**	**-40.9**		
S-14	Rio Penasco at HW 24	December-77	-8.20			
		April-78	-7.20			
		July-78	-9.10			
		March-01	**-8.18**	**-57.2**		
S-16	Rio Penasco at Elk, NM	March-01	**-8.17**	**-59.4**		
		August-01	**-7.80**	**-58.6**		
S-17	Rio Penasco at Mayhill	April-78	-9.70	-55.8		
		July-78	-9.60	-57.3		
		March-01	**-8.79**	**-62.4**		
		August-01	**-8.34**	**-62.4**		
S-21		March-01	**-7.80**	**-55.6**		
S-22	Eagle Creek at mile marker	March-01	**-8.33**	**-62.0**		Eagle Creek at mile marker 4, on HW
BL-1	Brantley Lake	August-01	**-6.45**	**-49.4**		
Snow Samples						
SN-1		March-01	**-6.92**	**-49.7**		sublimation??, collected at base of cloudcroft ski area
SN-2		March-01	**-9.20**	**-66.9**		Collected at mile marker 4 on the way up to ski apache

Note. Sample nomenclature is from Hoy and Gross (1982), which includes detailed information on sampling locations.
Sample values in bold were collected by M.Gabora as part of this study. The other samples were collected by Hoy and Gross (1982)

Appendix B. $\delta^{18}O$ versus time

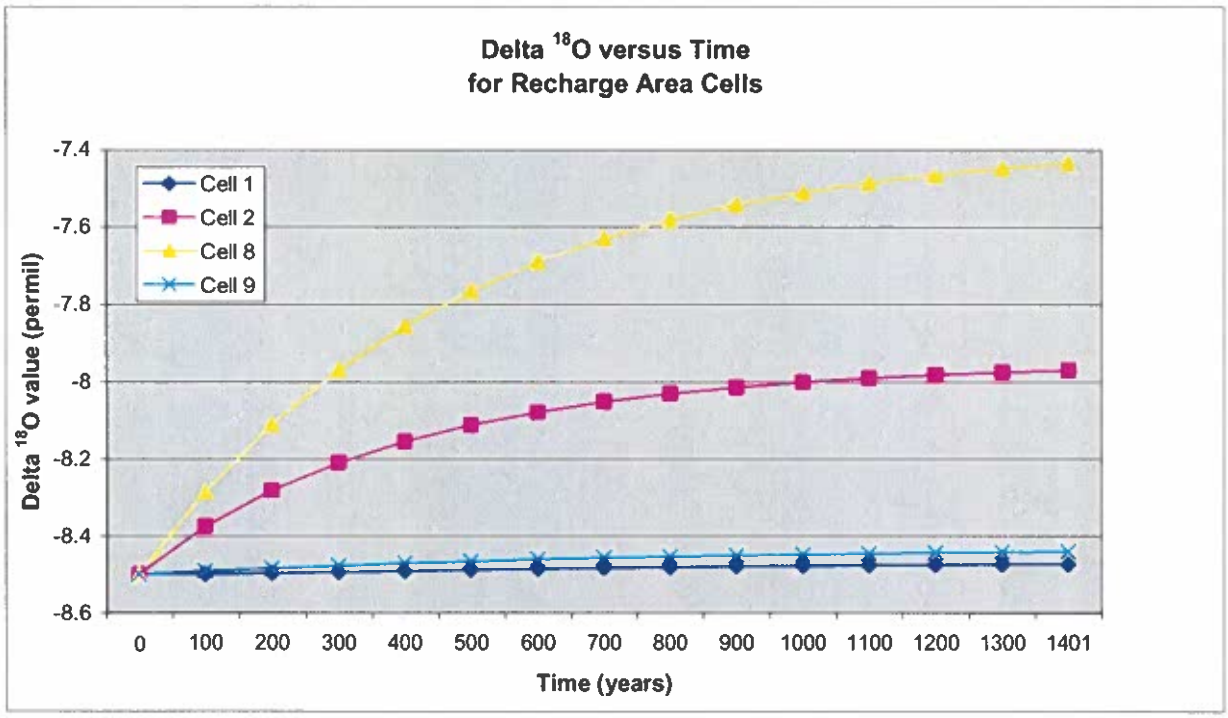
Delta 18O versus Time
for Recharge Area Cells
Cell 1
Cell 2
Cell 8
Cell 9
Delta 18O value (permil)
-7.4
-7.6
-7.8
-8
-8.2
-8.4
-8.6
0
100
200
300
400
500
600
700
800
900
1000
1100
1200
1300
1401
Time (years)

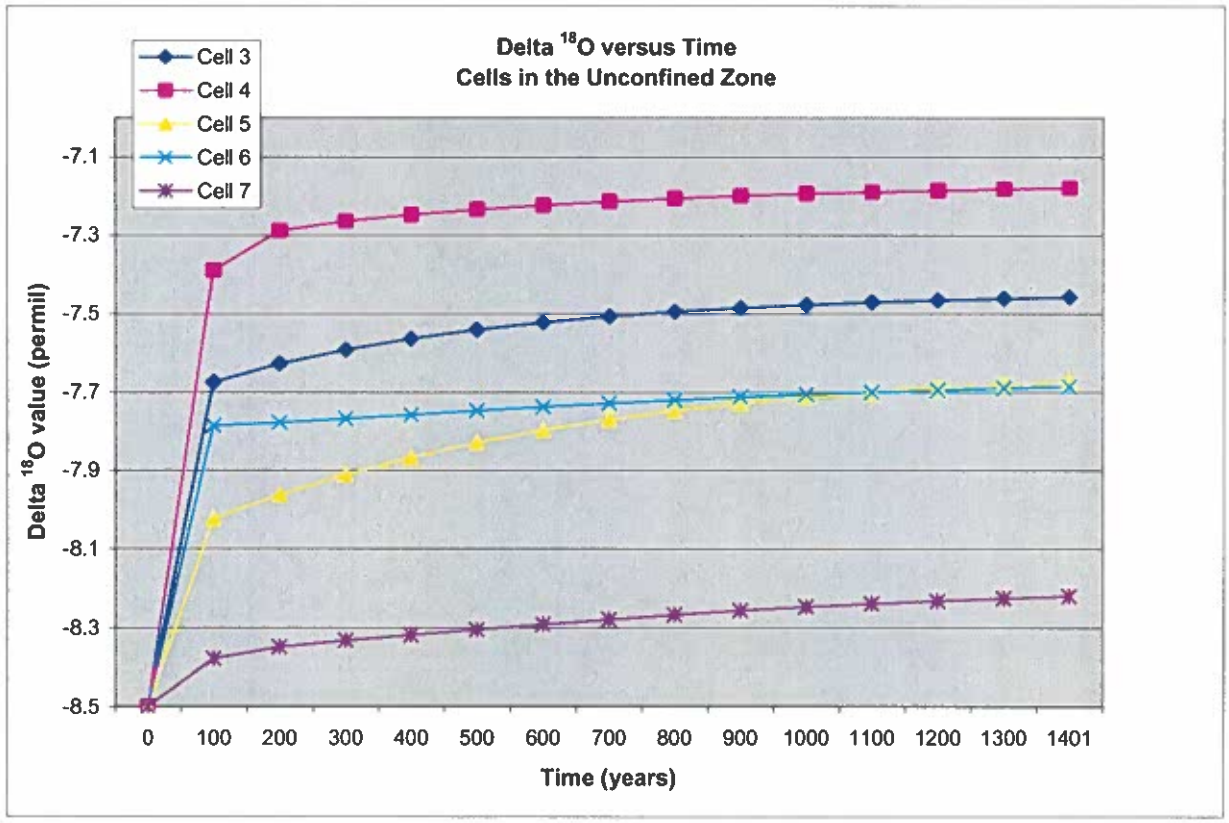
Delta 18O versus Time
Cells in the Unconfined Zone
Cell 3
Cell 4
Cell 5
Cell 6
Cell 7
Delta 18O value (permil)
-7.1
-7.3
-7.5
-7.7
-7.9
-8.1
-8.3
-8.5
0
100
200
300
400
500
600
700
800
900
1000
1100
1200
1300
1401
Time (years)

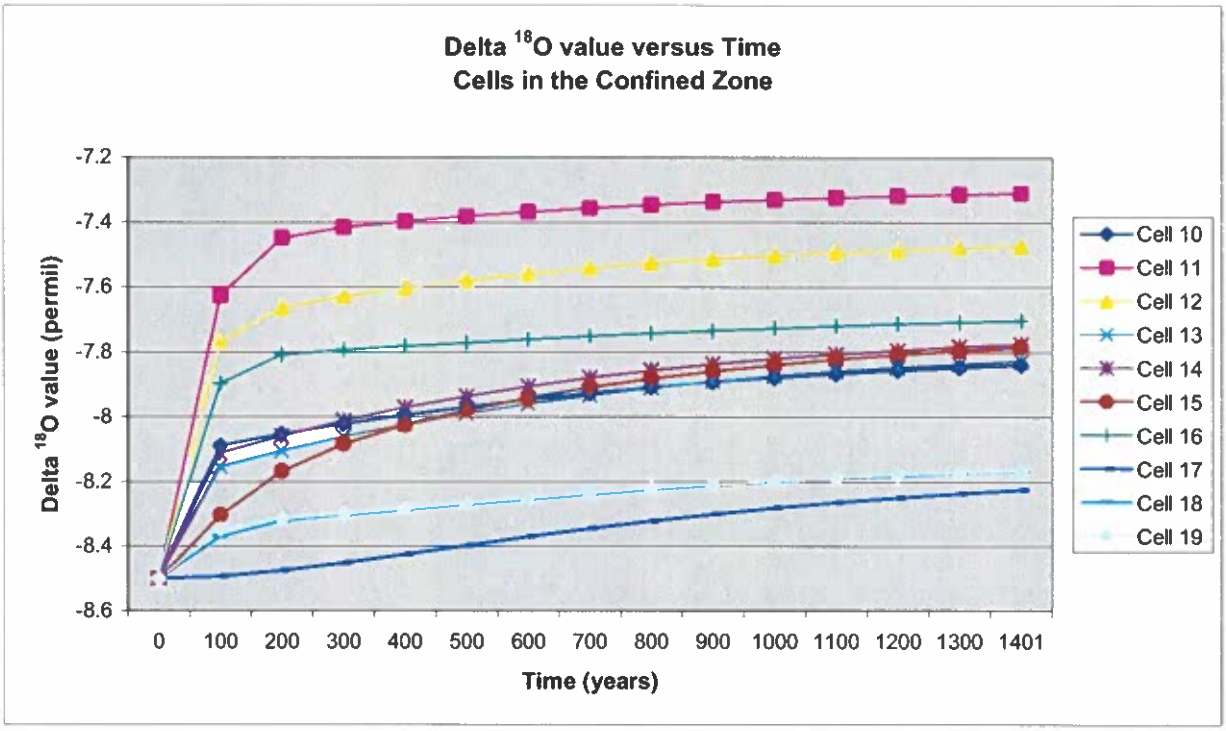
Delta 18O value versus Time
Cells in the Confined Zone
Delta 18O value (permil)
-7.2
-7.4
-7.6
-7.8
-8
-8.2
-8.4
-8.6
0
100
200
300
400
500
600
700
800
900
1000
1100
1200
1300
1401
Time (years)
Cell 10
Cell 11
Cell 12
Cell 13
Cell 14
Cell 15
Cell 16
Cell 17
Cell 18
Cell 19

Glossary

Artesian – Describes a state when water is under sufficient hydrostatic pressure to cause it to rise to the surface when the saturated media is penetrated by well.

Aquifer – A geologic formation that is sufficiently permeable to conduct groundwater and yield economically significant quantities of water to wells and springs

Carbonate – A sedimentary rock formed of the carbonates of calcium, magnesium and/or iron, e.g. limestone or dolomite

Cell – A subdivision of the mixing cell model having uniform properties such as effective porosity, unit thickness and target $\delta^{18}O$ value.

Confined - Groundwater that is under sufficient pressure to rise above the level at which it is encountered in a well. It may not flow to or above the ground surface (see Artesian) and its upper surface is a the bottom of a low permeability bed.

Confining Layer (bed) – A layer or material that is distinctly less permeable stratigraphically adjacent to one or more aquifers

Deuterium – A stable isotope of hydrogen that has one proton and one neutron in the nucleus.

Diffuse Recharge – Natural recharge derived from precipitation that falls on large portions of the landscape and percolates through the vadose zone to the aquifer.

Enriched – Of a relatively higher concentration, usually an isotope

Fractionation – The process by which on isotope is preferentially utilized as a result of differing bond strength

Isotope – One of two or more atoms, the nuclei of which have the same number of protons but different numbers of neutrons.

Karst (karstic) – The resulting geologic properties created by which the dissolution of limestone, dolomite or gypsum. Karst is characterized by sinkholes, caves and increased secondary porosity along fractures and bedding planes.

Leakage – The loss of water from geologic unit to another, such a canal infiltration along a river bottom

Radiogenic Isotope – A radioactive isotope of an element

Stable Isotope – An isotope of an element that does not radioactively decay

State – The mass of tracer in a cell

Steady – Does not change through time

Time Step – The time period represented by an iteration in the mixing cell model.

Tributary Seepage – When water infiltrates through a channel bottom and recharges the underlying aquifer

Tritium – A radioactive isotope of hydrogen that has one proton and two neutrons in the nucleus and has a half-life of 12.5 years.

Weighted Average – An average that reflects the relative importance of each quantities contribution.

List of abbreviations

δ – delta; expresses the mass difference of the sample from that of the standard and is equal to: $$\delta = \left(\frac{R_x - R_{std}}{R_{std}} \right) \times 1000$$

afy – acre-feet per year

BDC – boundary discharge concentration from a cell

BDV – boundary discharge volume from a cell

BRC – boundary recharge concentration into a cell

BRV – boundary recharge volume into a cell

C – concentration of tracer

d - day

dV/dt = time rate of change of volumetric storage in the system

ft - feet

GMWL – global meteoric water line

I – volumetric inflow

LMWL – local meteoric water line

m – meters

M – mass of tracer or state

MMC – modified mixing cell

MODFLOW – The USGS modular three dimensional finite-difference groundwater flow model

n –iteration number

O – volumetric outflow

List of abbreviations (con't)

OSE – Office of the State Engineer (New Mexico)

Q – flow

SBDC – system boundary discharge concentration

SBDV – system boundary discharge volume

SBRC – system boundary recharge concentration

SBRV – system boundary recharge volume

SMOW – standard mean ocean water

T – transmissivity

V- volume

W- width of cell perpendicular to flow

References cited

Bean, R.T. 1949. Geology of the Roswell Artesian Basin, New Mexico, and its relation to the Hondo Reservoir. New Mexico State Engineer Office Technical Report 9, p. 1-31.

Campana, M.E. 1975. Finite state models of transport phenomena in hydrologic systems. Ph.D. dissertation, University of Arizona, Tucson, 252p.

Campana, M.E., and E.S. Simpson. 1984. Groundwater residence times and recharge rates using a discrete state compartmental model and C-14 data. Journal of Hydrology 72, p.171-185

Craig, H., 1961. Isotopic variations in meteoric waters. Science, 133, p.1702-1703.

Childers, A., and G.W. Gross. 1985. The Yeso aquifer of the middle Pecos Basin, analysis and interpretation – Hydrogeological analysis of geophysical well logs from the Pecos Slope. New Mexico Institute of Mining and Technology Report H-16. 162p.

Daniel B. Stephens and Associates. 1996. Comprehensive review and model of the hydrogeology of the Roswell Basin. *Prepared for* New Mexico Office of the State Engineer.

Davis, P., R. Wilcox, and G.W. Gross. 1979. Spring characteristics of the western Roswell Artesian Basin. New Mexico Water Resources Research Institute Report 116, p. 93.

Duffy, C.J., L.W. Gelhar, and G.W. Gross. 1978. Recharge and groundwater conditions in the western region of the Roswell Basin. New Mexico Water Resources Research Institute Report 100, p.111.

Fetter, C.W. 1994. Applied Hydrogeology. Prentice-Hall, Inc. 691p.

Fielder, A.G., and S.S. Nye. 1933. Geology and ground-water resources of the Roswell Artesian Basin, New Mexico. U.S. Geological Survey Water-Supply Paper 639. 372p.

Gross, G.W., P. Davis, and K.R. Rehfeldt. 1979. Paul Spring – An investigation of recharge in the Roswell (NM) Artesian Basin. New Mexico Water Resources Research Institute Report 113, 135p.

Gross, G.W. and R.N. Hoy. 1980. A geochemical and hydrological investigation of groundwater recharge in the Roswell Basin of New Mexico – Summary of results and updated listing of tritium determinations. New Mexico Water Resources Research Institute Report 122, 141p.

Hantush, M.S. 1957. Preliminary quantitative study of the Roswell groundwater reservoir, New Mexico. New Mexico Institute of Mining and Technology, Research and Development Division, 118p.

Hoy, R.N., and G.W. Gross. 1982. A baseline study of oxygen 18 and deuterium in the Roswell, New Mexico, Groundwater Basin. New Mexico Water Resources Research Institute Report 144, 95p.

Kelley, V.C. 1972. Geology of the Pecos county, southeastern New Mexico. New Mexico Bureau of Mines and Mineral Resources Bulletin 98, 55p.

Kirk, S.T., and M.E. Campana. 1990. A deuterium-calibrated groundwater flow model or a regional carbonate-alluvial system. Journal of Hydrology 119, p.357-388.

Lambert, S.S. 1978. Geochemistry of the Deleware Basin groundwater. Geology and mineral deposits of Ochoan Rocks in the Deleware Basin and adjacent areas (compiled by G.S. Austin), circular 159, p.33-38

Maddox,G.E. 1968. Geology and Hydrology of the Roswell Artesian Basin, New Mexico. University of Arizona Ph.D. dissertation.

McDonald, M.G., and A.W. Harbaugh. 1988. A modular three-dimensional finite-difference ground-water flow model. U.S. Geological Survey Techniques of Water Resources Investigations, Book 6, 586p.

Mourant, W.A. 1963. Water resources and geology of the Rio Hondo drainage basin, Chaves, Lincoln, and Otero Counties, New Mexico. New Mexico State Engineer Office Technical Report 28, 85p.

Poage, M.A., and C.P. Chamberlain. 2001. Empirical relationships between elevation and the stable isotope composition of precipitation: considerations for studies of paleoelevation change. American Journal of Science, v. 301, p. 1-15.

Rehfeldt, K.R., and G.W. Gross. 1982. The carbonate aquifer of the central Roswell Basin – recharge estimation by numerical modeling. New Mexico Water Resources Research Institue Report 142, 136p.

Rozanski, K., L. Araguas, and R. Gonfiantini. 1992. Relation between long-term trends of ^{18}O isotopic composition of precipitation and climate. Science, v.258, p.981-985

Sharp, Z., 2002. Class Notes, Stable Isotope Geochemistry. University of New Mexico.

Summers,W.K, 1972. Geology and regional hydrology of the Pecos River Basin, New Mexico. New Mexico Bureau of Mines and Mineral Resources Open-File Report 37, 208p.

Wasiolek,M., 1981. The hydrogeology of the Upper Rio Renasco Area between James and Cox Canyons in the Sacramento Mountains of southeastern New Mexico: M.S. Independent Study Report, New Mexico Institute of Mining and Technology, Socorro, New Mexico, p.138

Wasiolek, M. 1991. The hydrogeology of the Permian Yeso Formation within the upper Rio Hondo Basin and eastern Mescalero Apache Indian Reservation, Lincoln and Otero Counties, New Mexico. New Mexico Geological Society Guidebook, 42nd Field Conference, Sierra Blanca, Sacramento, Capitan Ranges. p.343-351

Welder, G.E. 1983. Geohydrologic framework of the Roswell ground-water basin, Chaves and Eddy Counties, New Mexico. New Mexico State Engineer Technical Report 42, 28p.